A Numerical Study on Combination of Crack Stop Hole and Carbon Fiber Reinforced Polymer (CFRP) Laminates as a Repair Technique

Jaswanthsai Vutkuru

A Thesis Submitted to

Indian Institute of Technology Hyderabad

In Partial Fulfilment of the Requirements for

The Degree of Master of Technology

Department of Civil Engineering

July, 2014

Declaration

I declare that this written submission represents my ideas in my own words, and where others' ideas or words have been included, I have adequately cited and adhered to all principles of academic honesty and integrity and have not misrepresented or fabricated or falsified any idea/data/fact/source in my submission. I understand that any violation of the above will be a cause for disciplinary action by the Institute and can also evoke penal action from the sources that have thus not been properly cited, or from whom proper permission has not been taken when needed.

_____

(Signature)

_____

(JaswanthsaiVutkuru)

_____

(CE12M1017)

This thesis entitled "**A Numerical Study on Combined Effect of Crack Stop Hole and Carbon Fiber Reinforced Polymer (CFRP) Laminates as a Repair Technique**" by **Jaswanthsai Vutkuru** is approved for the degree of Master of Technology from IIT Hyderabad.

Dr. S. Suriya Prakash
Internal Examiner

Dr. Viswanath Chinthapenta
External Examiner

Dr.Mahendrakumar Madhavan
Adviser

Prof. K.V.L. Subramaniam
Chairman

Acknowledgements

I would like to thank the Ministry of Human Resources Development (MHRD), Government of India for providing financial support during my stay at IIT, Hyderabad. During last one year time, the guidance and assistance given by my thesis advisor Dr. Mahendrakumar Madhavan is highly acknowledged. I would like to thank Dr. S.SuriyaPrakash, Dr. RamjiManoharan, and Prof. K.V.L. Subramaniam for reviewing the progress of my work. I am thankful for computational facilities provided by the department of civil engineering; IIT Hyderabad. I would like to thank my friends Mr.Vishwanath Sanap and Mr. Shashidar Reddy for their time and invaluable suggestions. I am thankful to my family, who helped me to pursue my Masters. I would like to thank Mr. JayaPrakashVemuri and Mr. Teja Dasari for their support during my stay at IIT Hyderabad.

List of Figures

List of Tables

Abstract

Drilling a hole ahead of crack tip is one of the most common techniques, to prevent further crack propagation in structures subjected to fatigue load. Fatigue cracks are typically occur at locations where drilling a crack stop hole of desired dimensions is not possible due to geometrical constraints. In such cases, crack may reinitiate from the hole after few loading cycles. Techniques such as Static mechanical cold working are used to strengthen the undersized crack stop hole mentioned in the literature. In this study, application of Carbon Fiber Reinforced Polymer (CFRP) patches laminated over cracks is proposed to delay the crack initiation from under sized crack stop hole.

Although extensive literature exists for crack stop hole and CFRP patches independently to prevent the crack growth, few literatures are available for combined effect. In the present study combination of crack stop hole and CFRP overlays as a repair technique is studied. This combination helps to reduce the stress at edge of the hole, which delays the crack initiation. The combined effect of crack stop hole and CFRP patches is studied numerically using ANSYS.

Steel plate subjected to tensile loading (mode-I) with initial central crack is considered. Material behaviour is assumed to be elastic. A hole is modelled ahead of crack tip and CFRP overlays are applied over it. Holes of various radii are considered to understand the effect of hole radii on stress at the edge of the hole. The entire setup is modelled in ANSYS. Ratio of stress intensity factor to square root of radius is $K_I/\sqrt{\rho}$considered as a parameter for all cases.By the application of CFRP patches, the $K_I/\sqrt{\rho}$ is reduced by 70% at a stiffness ratio of 0.16. It is also observed that at a stiffness ratio 0.95, the $K_I/\sqrt{\rho}$ value at the edge of the hole is reduced by 90%. A reduction parameter is proposed for $K_I/\sqrt{\rho}$ as a function of stiffness ratio.

In this study, it is observed that the parameter $K_I/\sqrt{\rho}$used for crack initiation, which is based on a constant stress gradient 0.5.This leads to smaller radius crackstop hole and hence is un- conservative. Therefore, another parameter called notch stress intensity factor (N-SIF) which takes into account the effect of stress gradient (α) is considered in determining the appropriate hole radius to halt crack propagation. This approach conservative compared to $K_I/\sqrt{\rho}$ approach.

Contents

Chapter 1

Introduction

1.1 Introduction

Steel bridge girders are subjected to fatigue loading due to continuous vehicular traffic. Girders which are not fabricated as per fatigue detailing may develop cracks due to fatigue load. In most cases, cracks initiate at potential sites like welds, where there is a material discontinuity. If the crack continues to grow and is left unrepaired for long time, it may lead to catastrophic failure, which is undesirable. Therefore cracks need to be arrested by using appropriate retrofitting techniques. By adopting the appropriate retrofitting techniques, the service life of the bridge can be increased. The success of any retrofitting technique depends on identifying the location of the crack and the nature of loading. These retrofitting techniques are classified broadly into two groups [Carol *et.al* (2004)] such as local and global retrofitting techniques. While the local retrofitting techniques modify the local stress state which includes crack stop holes, peening, gas tungsten arc (GTA) welding, the global retrofitting technique include strengthening with a steel plate or composite laminate.

Experimental studies by Fisher *et.al*, 1980 indicate that of the above discussed repair methods, drilling a crack stop hole ahead of a crack tip are one of the effective methods to arrest the crack propagation. The basic principle behind the crack stop hole is to convert the sharp crack into a blunt notch. The expression for the radius of the hole to be drilled is a function of both loading and material property. The success of this method depends on length of the crack, type of the loading and location of crack. In some cases, it is not possible to drill a hole with a radius as obtained from analytical expressions, due to lack of space in a complex structured steel connections. In such situations, a practicing structural engineer may be required to drill an undersized crack stop hole as a temporary measure. This approach may lead to re-initiation of crack stop hole after few loading cycles. Crack stop hole are fully effective only if the radius of the hole satisfy design requirements [Crain, 2010].

Crack stop hole technique is not feasible, if crack propagates to a substantial size. In such cases a global retrofitting technique such as external strengthening needs to be adopted. The usual practice was to weld an additional plate on the top of damaged portions. However, it was found that most of the cases, cracks were emanating from the edges of these attached plate. In addition, these plates were causing increase in dead load which was undesirable. Recently, Carbon Fiber Reinforced Polymer

(CFRP) plates have been used to replace these steel plates for external strengthening owing to its better properties such as light weight and better fatigue performance [Miller *et.al,* 2001].These techniques are more efficient and are applied in strengthening old bridges. In the current study, the combined effect of both these techniques i.e. drilling holes and application of adhesive patches are studied as repair techniques. The recent literature indicates a gap in the combined behaviour of crack stop hole and CFRP as a repair technique for retarding crack growth. From previous research, it was found that a new technique needs to be developed with the combination of drilling holes [Carol *et.al,* (2004)]. For repairing the cracks developed in bridge girders the guidelines given by Indian railways[Manual for Indian railway bridges (1998)] recommends drilling a 7mm diameter hole ahead of crack tip as a temporary measure and welding a plate over the crack as permanent solution to retard the crack growth.

1.2 Problem statement

Crack stop hole technique has limitations in some cases where it is not possible to drill a hole of calculated radius. It is observed in the literature [Andrea *et.al* (2001), Carol *et.al,* (2004)] that cracks are re initiating from the edges of the holes. The probable reasons for crack initiation at the edge of the hole are increase in load and mixed mode loading condition. However, there is a need to study crack reinitiating from the edge of the stop hole in detail. Two major expressions for radius of the crack stop hole are in literature; Barsom*et.al* (1971) and Fisher *et.al* (1980). Both these expressions consider the maximum stress ahead of the blunt crack tip given by Creagor and Paris (1967). The expression given by Barsom*et.al* (1971) is common for different grades of steel. The expression given by Fisher et.al is only for A36 steel. However, this study considers only two different diameters (1 in. and 0.5 in).If radius of the crack stop hole is undersized according to above mentioned studies, cracks will reinitiate after few loading cycles. In such case, to reduce the stress in the damaged component CFRP patches are applied on the top of damaged panel. The combined action of CFRP patch and crack stop hole is the main focus of the current study. To demonstrate this combined action a central cracked specimen geometry which replicates the generally occurred cracks in girders is considered.

Finite element analysis of central crack middle tension specimen with five different crack stop hole radii is carried out to understand the effect of hole radius. In addition to the crack stop hole a CFRP patch is applied over the damaged panel. A numerical study will be carried out to obtain the combined effect of CFRP patches and drilling holes.

1.3 Contents

Chapter-1 gives the introduction to the retrofitting techniques, problem statement and objectives.Chapter-2 explains the background of expressions for crack stop hole and a brief review of previous experimental studies of CFRP-steel applications. Different approaches for predicting the fatigue crack initiation life are presented. Among these approaches, Fracture mechanics approach for fatigue crack initiation is explained in detail. The concept of SIF and notch stress intensity factor (N-SIF) is introduced.Chapter-4; finite element modelling illustrates the modelling part of this study. Modelling of different geometriesChapter-5, gives details of results obtained.

Chapter 2

Background

2.1 Introduction

Drilling holes ahead of crack tip is one of the oldest techniques to stop crack propagation. This technique is sensitive to the hole radius. If the hole is small, the crack may reinitiate from the edge of the hole after a few loading cycles. At the same time, if the hole is bigger it will reduce the stiffness of the member. Hence it is important to drill the optimum size of the hole. To arrive at the hole radius, predicting the crack re-initiation from the edge of the hole is important. The existing expressions [Barsom*et.al* (1971), Fisher *et.al* (1980)] predict the hole radius based on a threshold value of $\Delta K_I/\sqrt{\rho}$ behind which crack initiation not takes place.

2.2 Fatigue crack initiation life for blunt notches

Fatigue is defined as the process of cumulative damage caused by repeated loading. Fatigue life of any structural steel component subjected to fluctuating load is divided into two parts: (a) Crack initiation life (N_i) (b) Crack propagation life (N_p) [Barsom and Nicol, 1974]. In order to determine the total fatigue life of the component these two parts needs to be calculated individually. Total fatigue life of the component is the sum of crack initiation and propagation life. For sharp cracks, the initiation life is negligible and the fatigue life of such components is equal to the fatigue crack propagation life. However, for blunt cracks the fatigue crack initiation life is significant and cannot be neglected. To predict fatigue life of a component, mainly three different approaches are available. They are stress life, strain life and fracture mechanics approach.

2.3 Stress life approach

In stress approach the test results presented using S-N curves. In S-N curves, S represents maximum stress and N represents cycles for failure. This data is obtained by testing polished specimens at various load magnitudes. The stress corresponding to infinite number of cycles is defined as fatigue endurance limit. A typical S-N curve for A517 steel is shown in Fig.2-1. If a component is subjected to a load less than endurance limit, it will have infinite fatigue life. Large test data on various steels indicate that the fatigue endurance limit is in the range of half the tensile strength of the component [Barsom and Rolf, 1999]. However, presence of notches or crack like discontinuities will reduces the endurance limit compared to that of a polished specimen. To account

this notch effect a reduction factor is introduced Eqn. 2-1. This reduction factor (K_f) is useful to determine the effective stress range.

$$k_f = \frac{\sigma_{D,s}}{\sigma_{D,n}} \quad (2\text{-}1)$$

Where,

$\sigma_{D,s}$= Endurance limit of smooth specimen

$\sigma_{D,n}$= Endurance limit of notched specimen

$$\Delta\sigma_{ef} = k_f * (\Delta\sigma_g) \quad (2\text{-}2)$$

$\Delta\sigma_{ef}$ = Effective stress range

$\Delta\sigma_g$= Gross stress range

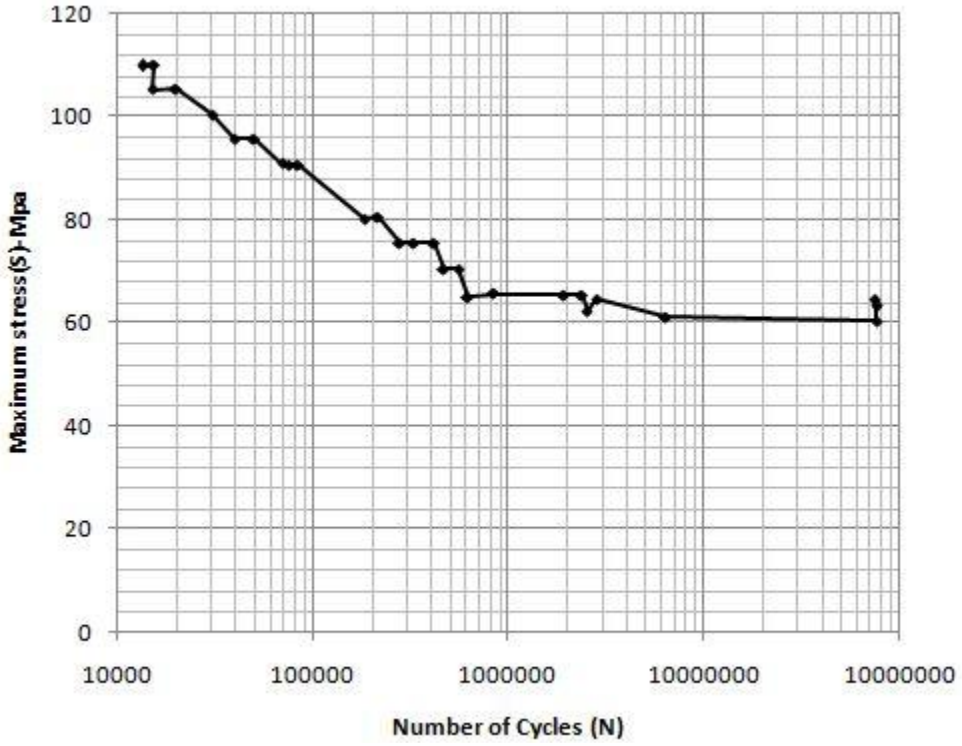

Figure 2-1 S-N Curve for polished specimens of an A517 steel obtained from rotating beam test (Barsom and Rolf, 1999)

The plastically deformed metal in the vicinity of notch tip in an elastically loaded structure leads to crack initiation. To model the localized plastic zones the specimens are tested under strain control. The specimen sizes are in the order of yield zone size to replicate the effect of yield zone. This approach is difficult to apply as there is no direct relation to applied loads.

2.4 Fracture mechanics approach

In the stress life approach, it is not possible to predict the crack propagation life. It is also not possible to delineate the crack initiation and propagation. Fracture mechanics approach overcomes this difficulty. Using fracture mechanics approach, the crack propagation life can be predicted. In this study, linear elastic fracture mechanics (LEFM) approach is adopted to explain the crack initiation from blunt cracks. To study the fatigue crack initiation from blunt notches, experimental studies were carried out by Barsom and Nicol (1974), Jack and Price (1970). Both studies express the fatigue crack initiation life (Ni) of the blunt crack, as a function of ratio of stress intensity factor fluctuation (ΔK) to square root of notch radius (ρ).

2.5 Stress Intensity Factor (SIF)

When a structural component with a crack is subjected to tensile loading, the value of stress at the crack tip is infinite. A parameter is required to describe the stress field near the crack tip. Stress Intensity Factor (SIF), proposed by Irwin (1958) is the parameter to describe the stress state near the crack tip. SIF is defined as a function of applied stress (σ) and square root of crack length (a). SIF is also a function of geometry of structural component, size and shape of the crack. The important feature of SIF is that, it relates the local stress field to applied far field stress. Typically, structural components subjected to fatigue loading experience mode-I deformation. Therefore, in present study mode-I deformation was considered. The well known expression for SIF for mode-I loading is given in Eqn.2-3. Here $F(\frac{a}{W})$ indicates geometric correction factor. The SIF is considered as a driving force for crack propagation.

$$K_I = \sigma\sqrt{\pi * a} * F(\frac{a}{W}) \qquad (2\text{-}3)$$

Near crack tip stress field equations for central cracked specimens are expressed as a function of SIF (K_I). The central crack geometry is as shown in Fig.2-2.

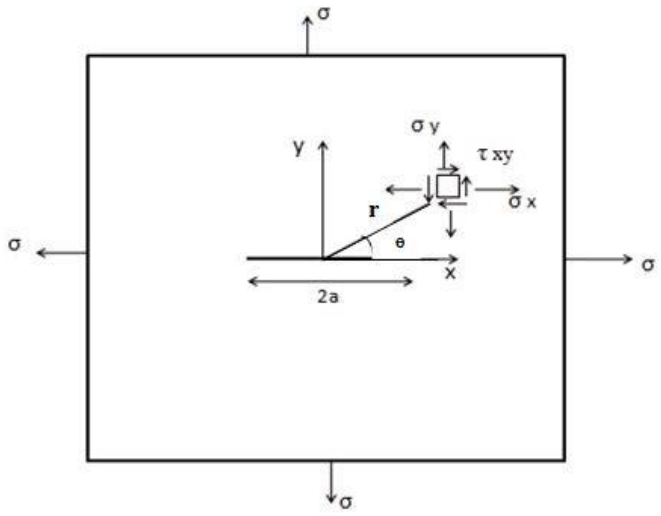

Figure 2-2 Elastic stress field distribution near the tip of mode-I

$$\boldsymbol{\sigma_x = \frac{K_I}{\sqrt{2\pi r}} \cos\frac{\theta}{2}\left(1 - \sin\frac{\theta}{2}\sin\frac{3\theta}{2}\right)} \quad (2\text{-}4)$$

$$\sigma_y = \frac{K_I}{\sqrt{2\pi r}} \cos\frac{\theta}{2}\left(1 + \sin\frac{\theta}{2}\sin\frac{3\theta}{2}\right) \quad (2\text{-}5)$$

$$\tau_{xy} = \frac{K_I}{\sqrt{2\pi r}} \cos\frac{\theta}{2}\sin\frac{\theta}{2}\sin\frac{3\theta}{2} \quad (2\text{-}6)$$

From the above stress field equations, it is clear that all these equations are function of stress intensity factor (SIF). SIF is a function of crack geometry, loading. Hence, the above stress field equations are same regardless of crack geometry and loading.

2.6 Stress field for blunt notches

Determination of $\Delta K_I/\sqrt{\rho}$ is important for predicting the crack initiation. In all above mentioned studies, the value of $\Delta K_I/\sqrt{\rho}$is expressed as a function of stress at the edge of the notch. The expression for stress field for sharp cracks was extended to blunt notches by Creager and Paris (1967). According to them, the notches were assumed as elliptic or hyperbolic (see Fig.2-3). The maximum stress at the edge of the notch according to Creagor and Paris is given in Eqn. 2-7.This equation is rearranged to express the $K_I/\sqrt{\rho}$ in terms of maximum stress.

$$\sigma_{max} = \frac{2K_I}{\sqrt{\pi\rho}} \quad (2\text{-}7)$$

$$\frac{K_I}{\sqrt{\rho}} = \frac{\sigma_{max}\sqrt{\pi}}{2} \quad (2\text{-}8)$$

The finite element analysis conducted in this study indicates that the Eqn.2-7 is able to predict the stress within 10% error up to a radius 0.2in.(4.57 mm). This is in agreement with finite element analysis conducted by Wilson and Gabrielse (1971). However, the radius of the hole drilled is in the range of 0.25 in to 0.5 in (Fisher et.al, 1980).

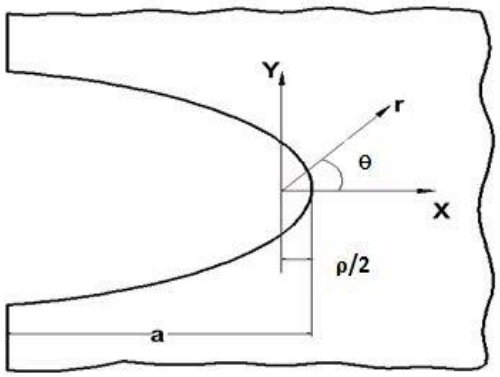

Figure 2-3 Shape of the notch (Creager and Paris assumption)

2.7 Crack initiation life for blunt cracks

Crack initiation life (Ni) for blunt notches is expressed as a function of ratio of SIF range (ΔK_I) and square root of notch radius (ρ). Experimental studies by Barsom and Nicol (1974), Jack and Price (1970) established this approach and expresses the fatigue initiation life as a function of $\Delta K_I/\sqrt{\rho}$. In low cycle region, the relation between radius of the notch (ρ) and $\Delta K_I/\sqrt{\rho}$ was given by Barsom and Nicol, 1974 (Eqn-2-9). In the low cycle region, for a given value of $\Delta K_I/\sqrt{\rho}$, the fatigue crack initiation life (Ni) is proportional to the square of notch tip radius (see Fig.2-4).

$$N_i = \frac{\beta}{\left[\frac{\Delta K_I}{\sqrt{\rho}}\right]^n} \quad (2\text{-}9)$$

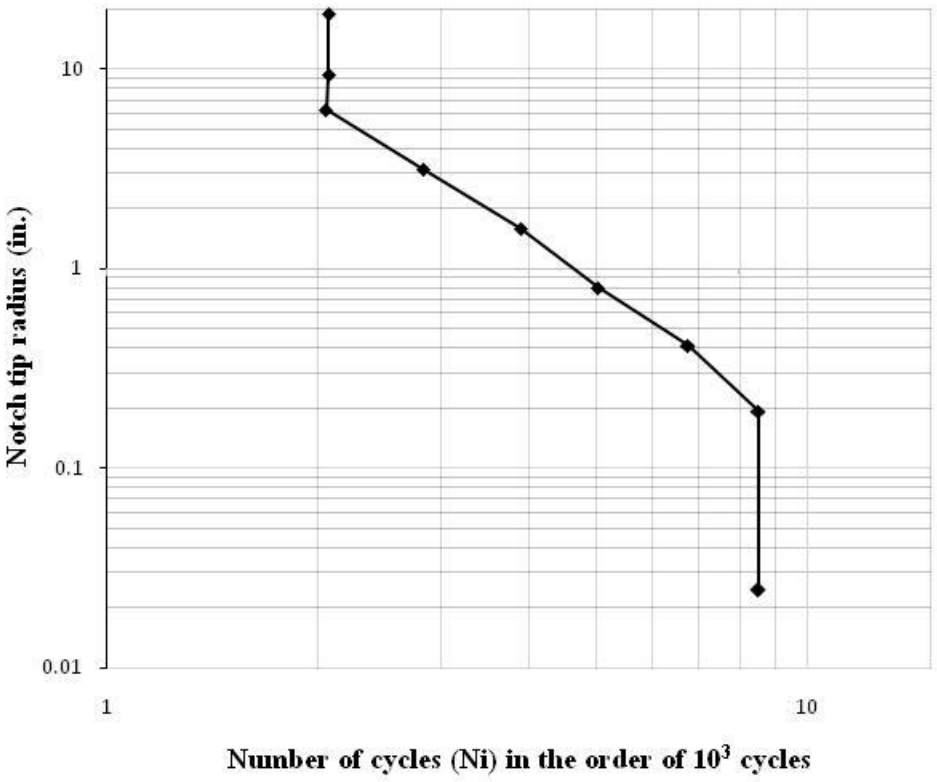

Figure 2-4 Cycle fatigue behaviour (Barsom and Nicol, 1974)

For notches with radius less than 0.01 in (0.254 mm), the crack initiation life (Ni) of the notch is independent of radius (see Fig.2-4). The same was also observed by Jack and Price (1971). The variation of crack life with radius can be explained on the basis of plastically deformed volume. As the radius of notch increases, the volume of plastically deformed material decreases, this leads in the delay of crack initiation. Foreman, 1972 studied experimentally the behaviour of crack initiation from flaws. In this study, the ratio of notch radius (r) to yield zone radius (w) was considered as a parameter to predict the crack initiation from blunt notches.

2.8 Radius of crack stop hole

To arrive at the size of the crack stop hole, fracture mechanics approach was adopted in previous studies [Barsom (1971), Fisher *et.al* (1980)].According to fracture mechanics approach, the crack initiation life (Ni), was expressed as a function of ratio of Stress intensity factor fluctuation (ΔK_I) fluctuation to square root of hole radius as shown in Eqn. 2-13. The relationship between two terms, $\Delta K_I/\sqrt{\rho}$ and maximum stress at the edge of the hole (σ_{max}) was given by Creagor and Paris [Creagor and Paris (1967)] using the concepts of linear elastic fracture mechanics (LEFM). These expressions were obtained by shifting the origin to a distance half of the radius ($\rho/2$) behind the crack front(see Fig.2-5), and is accurate when radius of the

hole is very less compared to the length of the crack (ρ<<a). The stress at the edge of the hole from where fatigue crack may reinitiate was obtained by substituting r= ρ /2 and ϴ=0.

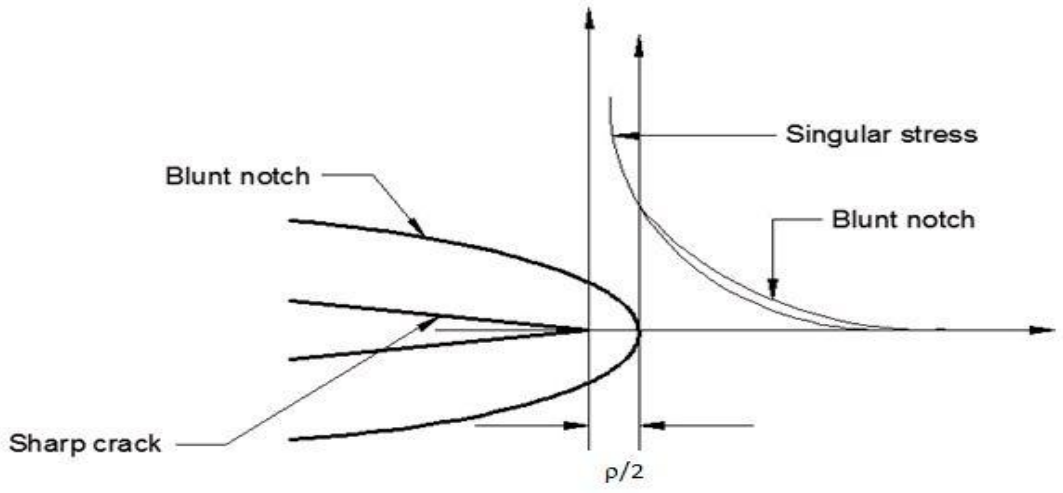

Figure 2.5 Stress field ahead of blunt notch

$$\sigma_x = \frac{K_I}{\sqrt{2\pi r}}\cos\frac{\theta}{2}\left(1 - \sin\frac{\theta}{2}\sin\frac{3\theta}{2}\right) - \frac{K_I}{\sqrt{2\pi r}}\frac{\rho}{2r}\cos\frac{3\theta}{2} \quad (2\text{-}10)$$

$$\sigma_y = \frac{K_I}{\sqrt{2\pi r}}\cos\frac{\theta}{2}\left(1 + \sin\frac{\theta}{2}\sin\frac{3\theta}{2}\right) + \frac{K_I}{\sqrt{2\pi r}}\frac{\rho}{2r}\cos\frac{3\theta}{2} \quad (2\text{-}11)$$

$$\tau_{xy} = \frac{K_I}{\sqrt{2\pi r}}\cos\frac{\theta}{2}\sin\frac{\theta}{2}\sin\frac{3\theta}{2} - \frac{K_I}{\sqrt{2\pi r}}\frac{\rho}{2r}\sin\frac{3\theta}{2} \quad (2\text{-}12)$$

$$\sigma_x = 0,\ \sigma_{max} = \frac{2K_I}{\sqrt{\pi\rho}} \quad (2\text{-}13)$$

2.9 Crack stop hole expressions

There are two major expressions existing in the literature, given by Barsom*et.al* (1971) and Fisher *et.al* (1980). Both researchers adopted fracture mechanics approach to explain their experimental studies on notches with different acuities. However, these two studies are different in terms of scale of testing and grade of steels used.

Barsom*et.al* (1971):

Notch effects in fatigue crack initiation behaviour of different grade steels From 250 Mpa(36 Ksi) to 800 Mpa (110 Ksi) were studied at stress ratio 0.1, in three point bending. The specimenwas single edge notched specimen as shown in Fig 2-6. They had found the fatigue crack initiation threshold $\left(\Delta K_I/\sqrt{\rho}\right)_{th}$ for different types of steel and it increases with the increase in grade

of the steel as shown in Fig 2-7. The same test carried out at different stress ratios between -1.0 and 0.5 indicate that the fatigue crack initiation threshold $\left(\Delta K/\sqrt{\rho}\right)_{th}$ is independent of stress ratio.

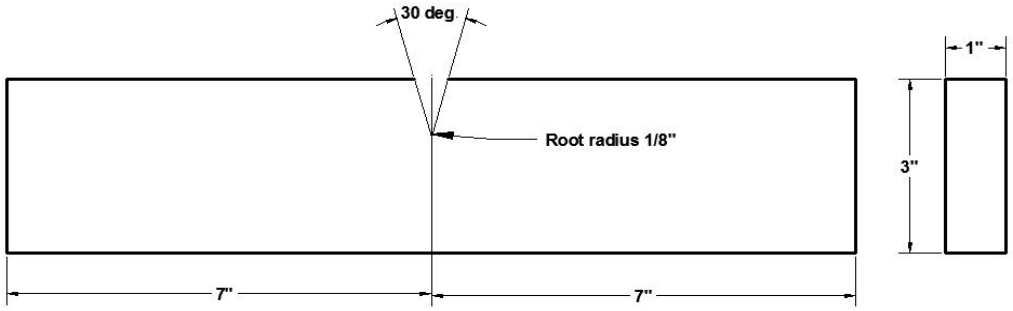

Figure 2-6 Single edge notched specimen (Barsom et.al, 1971)

The results of experimental studies by Barsom et.al indicate that for different grades of steel $\left(\Delta K/\sqrt{\rho}\right)_{th}$ is expressed as 10 times the square root of yield stress of the steel (σ_{ys}). The Eqn. 2-14 is unit sensitive and all units must be in Ksi and inches.

$$\frac{\Delta K_I}{\sqrt{\rho}} = 10\sqrt{\sigma_{ys}} \qquad (2\text{-}14)$$

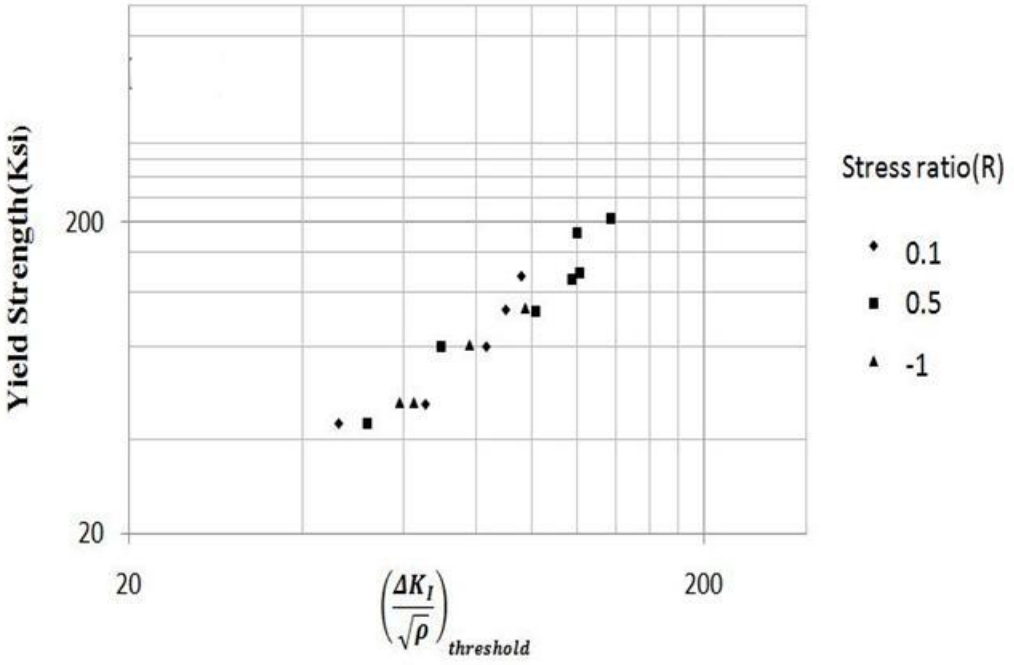

Figure 2.7 Effect of stress ratio on fatigue crack initiation threshold (Barsom et.al, 1971)

Fisher *et.al* (1980):

In their study, various retrofitting techniques were compared experimentally. These retrofitting techniques include peening, Gas Tungsten Arc welding (GTA) and crack stop holes. A comparison was made between different retrofitting techniques in terms of increase in fatigue life. For long cracks, a crack stop hole of 13mm (1/2 in.) and 25 mm (1 in.) diameter was drilled at the crack tips. After drilling crack stop hole, the radius of crack tip becomes radius of the hole.Tests were conducted at different stress ranges from41.2 Mpa to 103.4 Mpa. Figure 2-8 describes the loading condition, crack geometry and weld attachment used in their experimental study.

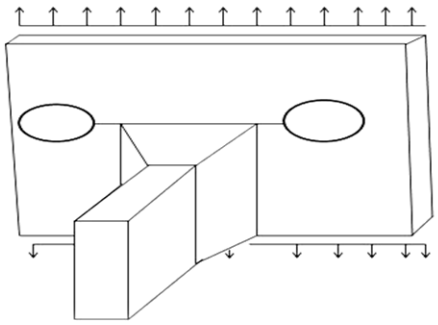

Figure 2-8 Specimen Geometry (Fisher et.al, 1980)

The results presented on a log-log scale included both thin and thick attachments (see Fig. 2-9). From this study Fisher *et.al* (1980) concluded that in case of bridge girders with weld attachments the threshold limit for crack initiation $(\Delta K_I/\sqrt{\rho}\,)_{th}$ should be limited to $10.5\sqrt{\sigma_{ys}}$. Eqn.2-15 is unit sensitive and the value of ΔK_I and σ_{ys} should be in Mpa$\sqrt{\text{mm}}$, Mpa.

$$\frac{\Delta K_I}{\sqrt{\rho}} \leq 10.5\sqrt{\sigma_{ys}} \qquad (2\text{-}15)$$

The Eqn.2-15 is converted for imperial (Ksi) units (Eqn.2-16). From this equation the threshold given by Fisher *et.al* shall be compared with the one given by Barsom and Rolf. Fisher et.al threshold is predicting higher radius value due to the effect of weld attachments which are not considered in the Barsom and Rolf expression.

$$\frac{\Delta K_I}{\sqrt{\rho}} \leq 4\sqrt{\sigma_{ys}} \qquad (2\text{-}16)$$

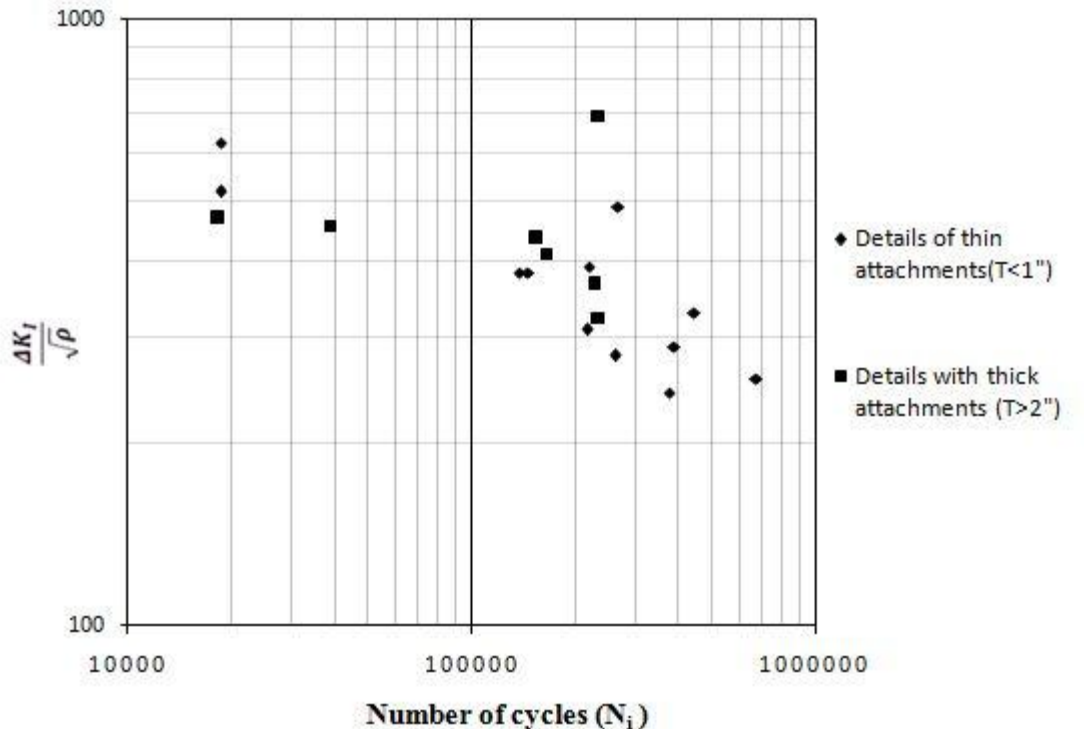

Figure 2-9 Crack initiation threshold results (Fisher *et.al*, 1980)

2.10 Limitations of crack stop hole

Crack stop hole technique has been used to prevent the crack propagation in bridge girders. However, effectiveness of crack stop hole is especially in case of distortion induced fatigue cracks, where the technique is not effective [Andrea *et.al*, 2004]. Andrea *et.al* (2004) examined this in a multi girder bridge which was replaced due to clearance demands. Over 300 distortion induced fatigue cracks were identified in the web gap region of diaphragm connections. One important observation in this study was the initiation of cracks from the crack stop holes drilled in the past. It was found that fatigue cracks in web gap region were result of combined effect of mode-I (Crack opening mode) and mode-III (Tearing Mode). Apart from distortion induced cracking, there are some instances where crack stop hole is not a feasible repair technique. The expression for radius of crack stop hole Eqn.2-17is directly proportional to square of applied stress dependent on magnitude of stress. For example, in case of mild steel ($\sigma_{ys} = 250$ Mpa) at a stress 5 percent yield stress, the design radius will be 10 percent of crack length (a). If the stress is 50 percent of yield stress then the radius will be 100 percent of crack length, which is not feasible to apply in the field.

$$\rho = \left(\frac{\Delta K_I}{10\sqrt{\sigma_{ys}}}\right)^2 \qquad (2\text{-}17)$$

2.11 Notch stress intensity factor (N-SIF)

Fatigue crack initiation is a function of stress range, average stress, material, and stress gradient. The SIF expression for blunt notches given by Creagor and Paris in mode-I Eqn. 2-13, considers the stress at a characteristic distance X_c ahead of notch tip. This expression Eqn.2-13 is only a function of notch tip radius. The stress gradient, which also effects the crack initiation, is not considered in this expression.

$$K_I = \sigma_{yy}(X_C)\sqrt{\pi X_C}\frac{\left(2+\frac{\rho}{X_C}\right)^{3/2}}{2\left(1+\frac{\rho}{X_C}\right)} \qquad (2\text{-}18)$$

To account for stress gradient, a parameter called notch stress intensity factor (N-SIF) is defined [Boukharouba et.al, 1995]. N-SIF is based on stress distribution ahead of notch tip. The stress distribution can be divided into three regions. Figure 2-10 describes the stress distribution ahead of sharp V-notch.

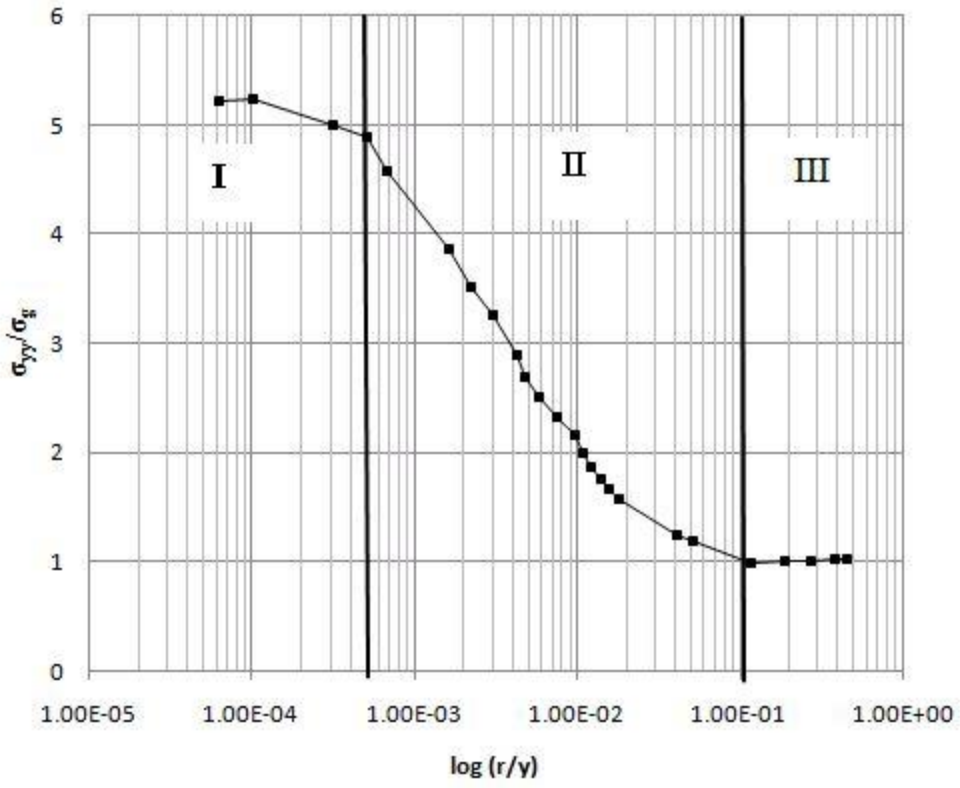

Figure 2-10 Stress distribution for sharp V-notch (Bukharouba *et.al,* 1995)

Region-I: The maximum stress is constant in this region. This region is defined up to a characteristic length (X_C). Characteristic length is defined as distance up to which stress remains constant.

Region-II: A Stress distribution is a straight line and slope of this line indicates the stress gradient.

Region-III: The magnitude of the stress is equal to nominal stress applied.

The stress distribution ahead of blunt notch is different from sharp notches up to some distance due to blunting. The stress at the crack tip will decrease due to blunting. The expression for N-SIF for blunt notches is given by Boukharouba*et.al*, 1995.

$$K_\rho = \sigma_{yy}(X_c) * \sqrt{2\pi}\left(X_c + \frac{\rho}{2}\right)^{\alpha} \quad (2\text{-}19)$$

In the Eqn. 2-11,

σ_{yy}= Stress at characteristic distance X_c

ρ= Radius of the notch

α= Stress gradient

2.12 Application of CFRP patches

Application of composite patches over damage panel is one of the crack retardation techniques. A.A Baker of Royal Australian air force pioneered the technique of using composite patches to repair the damaged components of aircraft (Baker, 1971). To arrive at the important parameters like bond behaviour, thickness of the patch Baker carried out a comprehensive study. In most of the cases Boron epoxy patches were implemented as a repair technique. A number of numerical studies were carried out in arriving at optimum patch dimensions by various researchers. The possibility of application of same technique for damaged bridge girders generated lot of research interest.

The application of CFRP to strengthen the damaged bridge girders was studied experimentally by Miller *et.al* (2001). To establish this repair technique, the parameters need to be studied are selection of materials, bond length and durability. Miller *et.al* (2001) established these parameters through experimental studies and applied CFRP patches to a damaged bridge girder. In this study the bridge girder was subjected load test by using a dump truck. The application of CFRP patches increased the global stiffness and strength of the girder.

2.13Bond length

In CFRP patch repair method, the bond length is an important parameter which affects the load transfer. To determine the bond length, the axial strain distribution along the CFRP patch length is considered as a parameter. The expressions for adhesive shear stress (τ_a), normal stress in the substrate (σ_s) and peel stress (σ_p) for double symmetric adhesive joint were obtained by using the linear elastic one dimensional solution (Hart-Smith, 1973). This approach was further extended to tapered joints and reinforcements by Albat and Romilly (1999). Miller *et.al* (2001) experimentally studied the bond length between steel plate and CFRP plate. The strain along CFRP patch length was measured and compared with the theoretical model. It was observed that 99% of load transfer takes place up to 4in (100 mm) development length. The bond behaviour and effective bond length studied by Fawzia*et.al*(2006) indicates the existence of effective bond length beyond which no significant load transfer takes place.

2.14Retrofitting the cracks emanating from notches using CFRP patches

The fastener holes, acts as crack initiators in air craft components. To strengthen these holes, static cold working technique is usually employed. In addition to cold working, CFRP patches were also used to strengthen these holes. Heller *et.al* (1989) carried out experimental study to find out the combined effect of adhesive patches and static cold working. The fastener holes were strengthened, so that the crack growth from the edges of hole decreases. The testing program involves two sets of specimens (1) fastener hole with edge notch strengthened using cold working, (2) fastener hole with both cold working and adhesive patches. From this experimental program concluded that strengthening with bonded adhesives in addition to bonded sleeve increases fatigue life by 2 times. Jones.C*et.al* (2003) carried out an experimental program to find the effect of different parameters ranging from surface preparation, development length, and single sided double sided patch applications on efficiency of patch system. Two types of specimens, central hole and edge notched were considered. This study, observed that application CFRP overlays are beneficial both as a preventive and repair technique. The important conclusion from this study is CFRP patches were effective in arresting the cracks originated from notches.

Tavakkolizadeh*et.al* (2003) conducted experiments on notched steel beams repaired with CFRP under four point bending load. CFRP patches were applied on tension flanges. He tested a total of 21 specimens of S127*4.5 A36 steel with CFRP patches. The results showed that the CFRP patch not only tends to extend the fatigue life of the component but also decreases the crack growth. A review of work done in strengthening of steel structures with composites was presented by Zhao

and Zhang (2006). This study indicated that bond behaviour, bond strength and fatigue crack propagation modelling are important study areas in this repair technique. From these studies the effectiveness of CFRP in strengthening the damaged steel bridge girders is established. However, the numerical study required to find out the various parameters of the patch repair system made it difficult for application. Zhao *et.al* (2008) came up with an analytical model to predict the fatigue crack propagation for cracks emanating from CFRP strengthened circular notches.

Achour*et.al* (2003) performed finite element analysis to understand the effect of composite patches in retarding the crack from semi circular notches. The stress concentration factor was decreased by 30% due to patch. The properties of patch system such as patch thickness and adhesive properties needs to be optimized for the effectiveness of the repair. Alemdar*et.al* (2012) conducted a detailed experimental program combined with finite element study to find out influence of different variables stiffness ratio, Young's modulus of composite, thickness of adhesive and no. of layers. It was concluded that stiffness ratio greater than one leads to diminishing result.

2.15 Summary

From the existing literature it is clear that adhesive patches are one of the most reliable repair techniques in aerospace engineering. Same technique applied to repair damaged bridge components. This technique proved to be successful and can be used with conjunction of old and simple repair technique such as drilling holes. Jones.C*et.al* (2003) experimentally demonstrated the effect of CFRP patches along with circular notch. Their study showed that fatigue life of the specimen increased by more than 50% when CFRP was applied over cracks emanated from central hole. Previous experimental studies conducted by various researchers proved that the combination of hole and composite patch are effective. However, there is a need to study the combined action of CFRP patch and hole both numerically and experimentally. In current study fracture mechanics approach is considered to study this combined action.

Chapter 3

Finite element modelling

3.1 Introduction

Finite element analysis (FEA) is conducted in this study using ANSYS 12.0 software. For modelling all components (i.e. steel plate, adhesive, and CFRP plate) Solid 186 element is used. Solid 186 element has mid side nodes and perform better in stress singularity regions. The bond between steel substrate and CFRP patches is assumed to be perfect and modelled as bonded contact by using multi point constraint (MPC) algorithm. Static tensile load is applied for all the analysis.

3.2 Specimen Dimensions

The mechanism of crack stop hole is to convert sharp crack into blunt notch. To illustrate the effectiveness of the notch different types of geometries were studied by previous researchers as shown in Fig.3-1.These geometries are useful in arriving at the optimum size of the hole to be drilled through experimental studies. However, due to practical difficulties, none of these geometries represent the real shape of crack stop hole. In current study the specimen geometry is considered in such a way that it represents the real shape of crack stop hole. The geometry of the plate is as shown in the Fig.3-2.The specimen geometry is taken from the experimental work of Barsom and Nicol (1974) and modified from double edge notch specimen to central crack specimen to model the effect of crack stop hole.

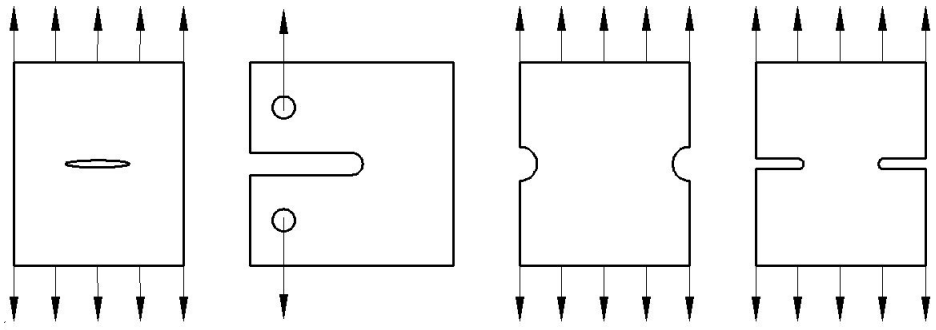

Figure 3-1 various notch geometries used in previous studies (Barsom and Rolf, 1999)

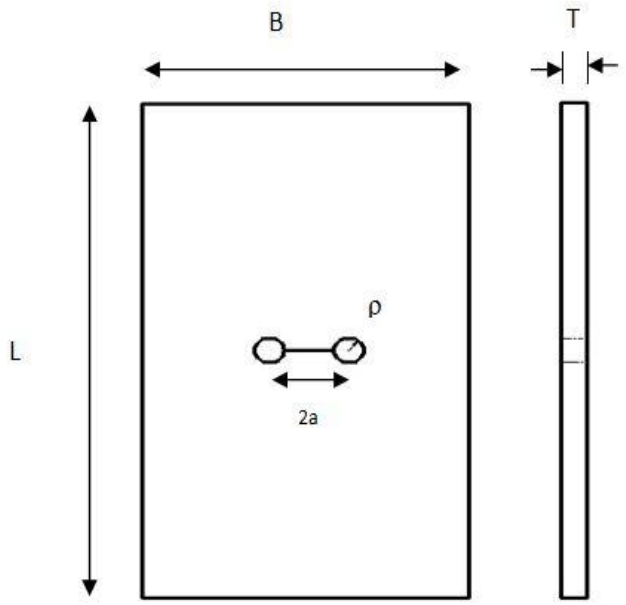

Figure 3-2Crack stop hole geometry

The dimensions of the geometry are given in Table 3-1. Five different radius (ρ) are considered in this study to find the effect of radius. Dotted line indicates the path considered for calculations.

Table 3-1 Dimensions of the specimen

Width of the specimen (b)	152.4 mm
Height of the specimen (l)	294.2 mm
Length of the crack(2a)	50.8 mm
Total length of crack (2a+2*ρ)	50.8+2* ρ mm
Thickness of the steel plate	3.175 mm

3.3 Modelling Plate geometry

To model the given geometry (plate geometry) 3-D SOLID 186 element is chosen from the list of ANSYS Library. This 20 nodded element has nonlinear material capabilities. SOLID 186 is also having mid side nodes and gives better results. Each node will have three translational degrees of freedom. Umamaheswar and Singh (1999) described that, for modelling this repair technique efficiently plate, adhesive and patch should be modelled as a solid elements with one brick thick. This is one of the most efficient modelling techniques as it will reduce the size effect. Linear elastic

material behaviour is considered. This assumption is needed as the expression for crack stop hole existing in the literature in terms of SIF, which is under linear elastic assumption. However, this assumption is valid in most of the cases due to the fact that most of the bridge girders loaded well below their yield strength. The solid 186 element is as shown in Fig.3-3. The nodes represented with alphabet and faces are represented with numbers.

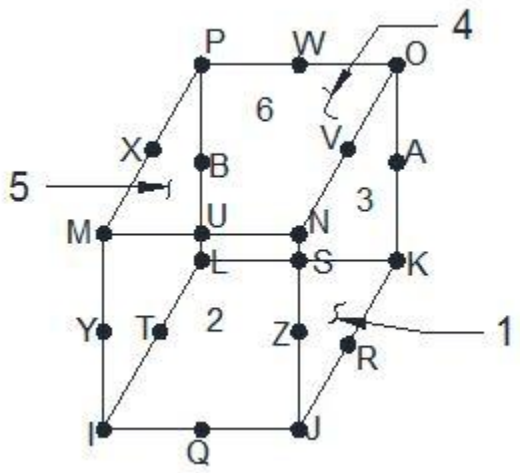

Figure 3-3 Solid 186 elements

Incremental meshing is employed around the hole to capture the sharp stress gradient. The value of stress at the edge of the hole is sensitive to element size (see Fig.3-5). For five different hole diameters considered in the study different element sizes are employed. Size of the element is decided for each radius based on change in stress value with the change of element size (see Fig.3-4). Six elements in thickness direction, 20 elements in radial direction, and 48 elements in angular direction (A total of 5760elements) are used around the hole.

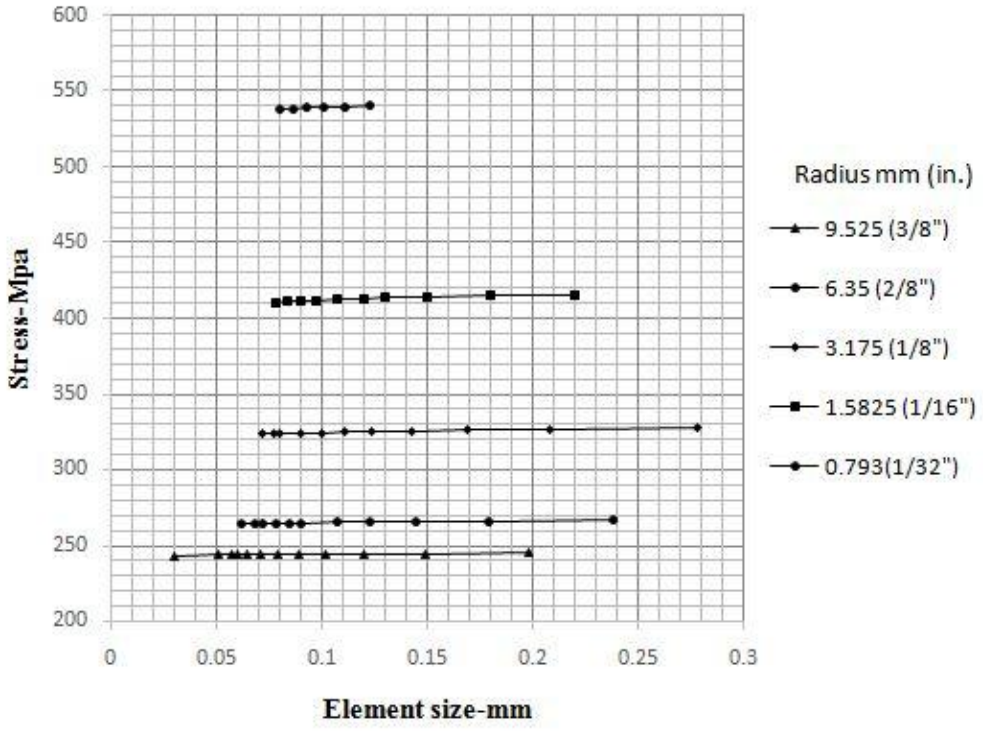

Figure 3-4 Element size Vs stress

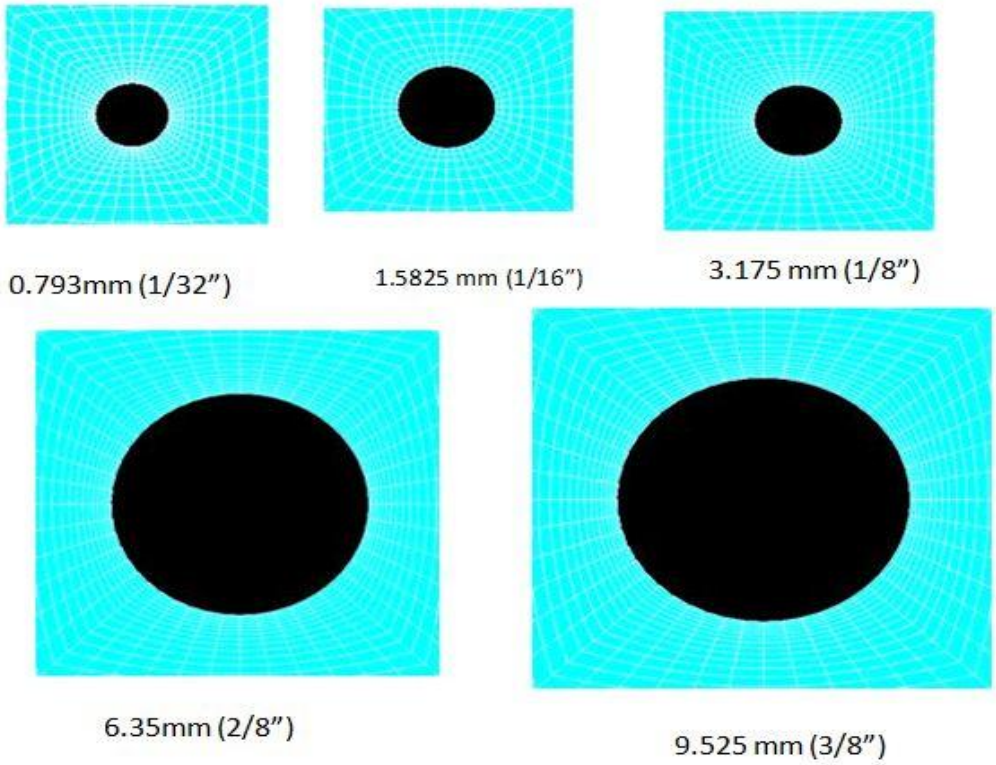

Figure 3-5 Finite element models with different radius

3.4 Material Model

The behaviour of steel is assumed to be linear elastic. The loading conditions, crack geometry are such that the material behaviour is linear elastic. For steel Young's modulus (E) value is taken as 200 Gpa and Poisons ratio (υ) as 0.3. However, to understand the non linear effects, three different loadings 62 Mpa, 82.7 Mpa, 103.4 Mpa are considered. Multi linear isotropic hardening (MISO) model is used to study the non linear behaviour of the material. MISO model is available in ANSYS 12.0 material model library. MISO model uses Von Misses failure criteria and isotropic hardening rule. This model is good for small strain problems. The stress strain curve for mild steel used in this study is given in Fig.3-6.

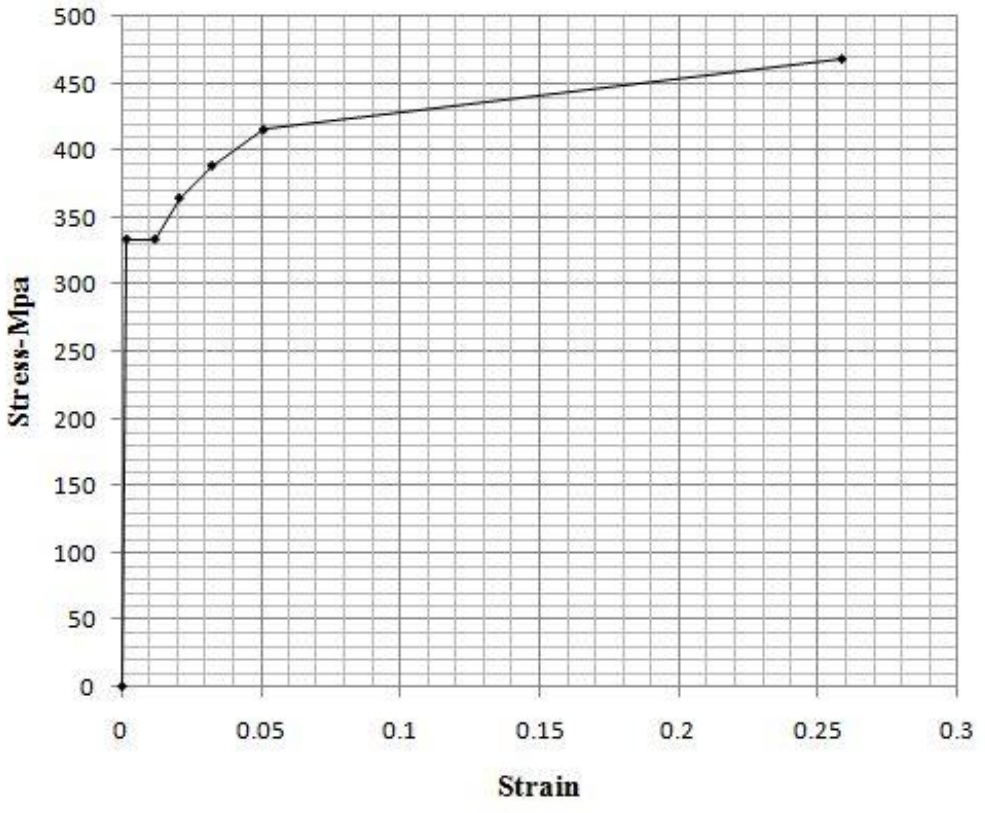

Figure 3-6 Stress strain curve for mild steel

Properties of CFRP laminate

CFRP laminate is modelled as an orthotropic material. CFRP material properties are taken from Ramji*et.al*(2012).Thickness of the lamina reported in the reference is 0.375mm.The properties of composite lamina are given in the Table 3-2.The finite element analysis conducted in this study

indicates that the Eqn.2-8 is able to predict the stress within 10% error up to a radius 0.2in.(4.57 mm). This is in agreement with finite element analysis conducted by Wilson and Gabrielse (1971).

Table 3.2 Material Propertied Used in this study Ramji*et.al*(2012)

Material	E_x (Gpa)	E_y (Gpa)	E_z (Gpa)	G_{xy} (Gpa)	G_{zy} (Gpa)	G_{xz} (Gpa)	υ_{xy}	υ_{zy}	υ_{zx}
Steel	200	_	_	_	_	_	0.3	_	_
Adhesive	4.97	_	_	_	_	_	0.47	_	_
CFRP	135	93	93	5	8	5	0.3	0.02	0.3

E: Young's modulus; G: shear modulus; υ: Poisson's ratio

3.5 Orientation of fibers

From previous studies it is learnt that to get the maximum effect fiber should be orientation in the direction of the load. In this case fibers are oriented 90^0 along the loading direction. However, to verify the model three different orientations are considered.

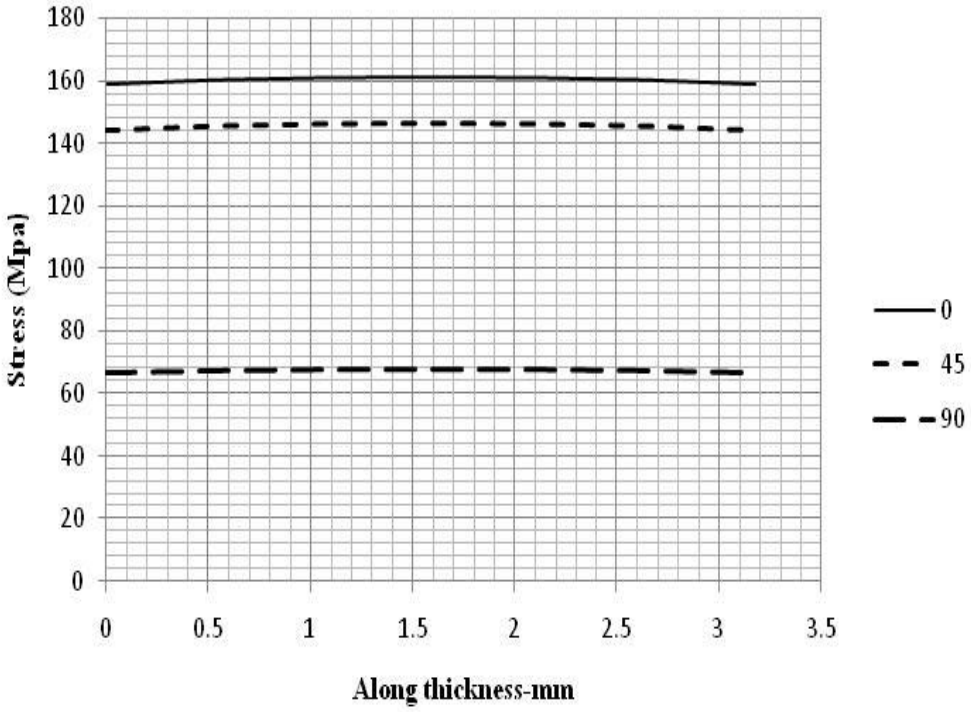

Figure 3-7 Fiber Orientation Vs Stress

To utilize the fiber strength effectively, fibers need to align in the direction of applied load. However, different fiber orientations are considered and analyzed. Among these three Orientations 90^0 patch layup gives more stress reduction. From Fig. 3-7 the through thickness stress reduction is more for 90^0 patch layup.

3.6 Bonded contact

The connection between CFRP, steel plate and CFRP, adhesive are modelled using bonded contact. In bonded contact, contacting surfaces are assumed to be glued together throughout the analysis. To create bonded contact, contact and target elements needs to be defined on the faces of elements, where they come into contact. In this study Multi point Constraint (MPC) algorithm is used for bonded contact. MPC connection is good for linear contact analysis. It will reduce the number of equations by eliminating the degrees of freedom for contact and target faces. Bonded contact especially MPC is useful in connecting the dissimilar meshes and it is preferred over the use of constraint equations.

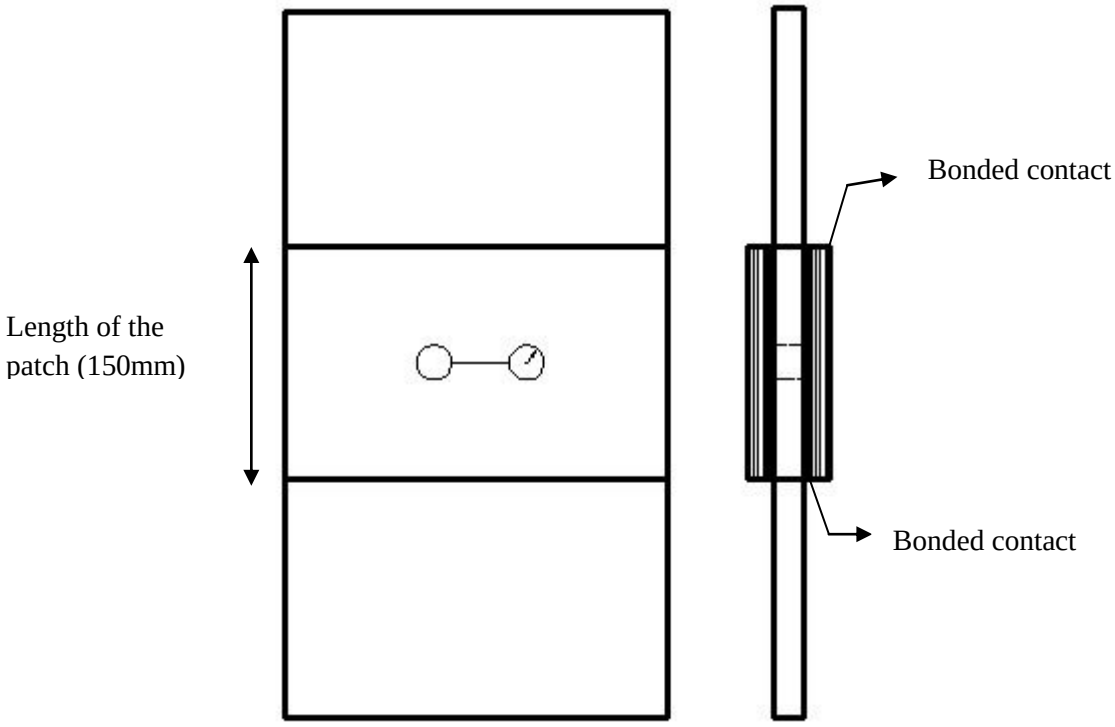

Figure 3-8 Multi point constraint (MPC) bonded contact

The following are the steps followed in the contact analysis:

1. The geometry of crack stop hole specimen and CFRP patches created
2. All geometries are meshed with solid 186 elements (see Fig.3-8)
3. A new contact pair is defined using contact wizard
4. A surface to surface contact is defined
5. Contact and target areas defined
6. A linear contact is used
7. MPC algorithm is selected for bonded contact.

Same steps are followed for all four contact pairs generated.

Chapter 4

Results and Discussions

4.1 Introduction

This numerical study is aimed at studying the combined action of crack stop hole and CFRP patch in arriving at appropriate crack stop hole radius when subjected to static tensile load. Prior to the combined effect, the effect of bare steel specimen was studied to understand the effect of hole radius in crack retardation. It was observed that the existing equations for crack stop hole was unconservative due to the fact that a constant stress gradient (α =0.5) was used irrespective of the hole radius. To study the combined action of CFRP patch and hole radius, various stiffness ratios were considered. In addition, non-linear analyses were also carried out to calculate the notch stress intensity factor (N-SIF).

4.2 Stress Distribution ahead of hole

The stress in distribution in the Y-direction (σ_{yy}) ahead of the crack stop hole and along the blunt edge (through thickness) are shown in Figs 4-1 (a) and (b).

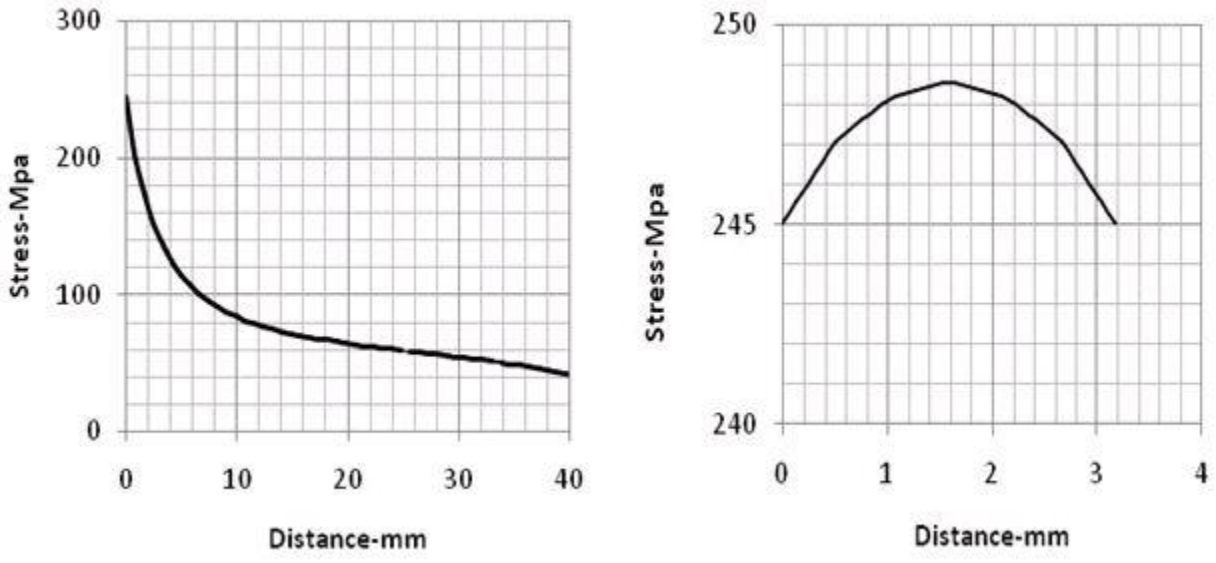

(a) Stress distribution ahead of hole

(b) Through thickness variation

Figure 4-1 Stress Distribution ahead of the hole

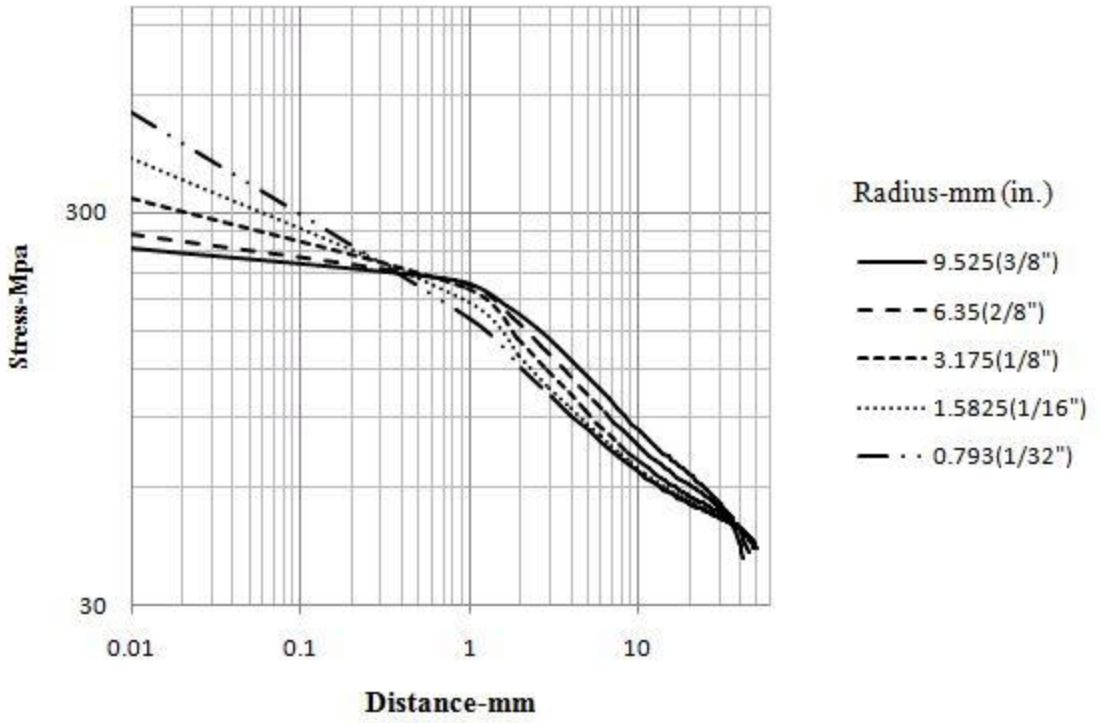

Figure 4-2 Stress variation ahead of hole

From Fig. 4-2, it can be observed that the value of maximum stress at the edge of the hole decreases as radius increases. By increasing the radius from 0.78 mm (1/32") to 9.37 mm (3/8"), the value of stress decreases by 54% at the hole edge. In addition, the stress gradient can be minimized by increasing the hole radius.

4.3 Fracture stress concentration factor(K_f)

The two major expressions available for crack stop hole (Barsom and Rolf (1971), Fisher *et.al* (1980)) are based on the Creager and Paris stress prediction for blunt notches. To demonstrate the accuracy of Creagor and Paris approach at different radius, fracture stress concentration factor (K_t) is calculated using Eqn.4-1. These values are compared with Stress Concentration factor from finite element analysis. The comparison is given in the Table 4-2.

$$K_f = \frac{2K_I}{\sigma\sqrt{\pi\rho}} \tag{4-1}$$

$$K_t = \frac{\sigma_{max}}{\sigma_{applied}} \tag{4-2}$$

The notch formed by drilling the hole is treated as a crack of length equal to the original crack length plus two times the radius of the hole (a+2*ρ). To calculate the stress intensity factor (K_I) for

(4-3)

central crack, the Eqn. 4-3 given by Paris and Sih (1965) is used. In Eqn.4-3, the dimensions of the crack stop hole geometry (see Fig.

$$K_I = \sigma * \sqrt{\pi a} \left(\frac{2b}{\pi a} \tan \frac{\pi a}{2b}\right)^{1/2}$$

In the above expression,

Length of the crack (2a) = (50+2* ρ) mm

Width of the plate (2b) =152.4 mm

Applied stress (σ) = 41.2 Mpa

Table 4.1 Calculation of Stress intensity Factor (SIF)

Radius of the hole ρ mm (inch)	Length of crack (a+2*ρ) (mm)	K_I (Mpa$\sqrt{mm}$)
9.56 (3/8")	69.8	630.80
6.35 (1/4")	63.5	551.93
3.17 (1/8")	57.15	480.61
1.58 (1/16")	53.97	447.28
0.79 (1/32")	52.38	431.11

The value of SIF (K_I) from Table 4.1 is substituted in Eqn. 4-1 to obtain the fracture stress concentration factor. The stress concentration factor (K_t) for different radii is presented in Table4-2. It can be observed from Table 4.2 that the regular stress concentration factor shows conservative results compared to fracture stress concentration factor.

Table 4.2 Comparison between K_f and K_t

Radius of the hole (mm)	Maximum Stress (Mpa)	K_f	K_t	$\frac{(K_f - K_t)}{K_t} * 100$
9.56 (3/8")	245	5.15	5.94	13.35
6.35 (1/4")	266	5.85	6.40	8.55
3.17 (1/8")	327	7.25	7.83	7.40
1.58 (1/16")	412	9.57	10.0	4.27
0.79 (1/32")	534	13.07	13.10	0.22

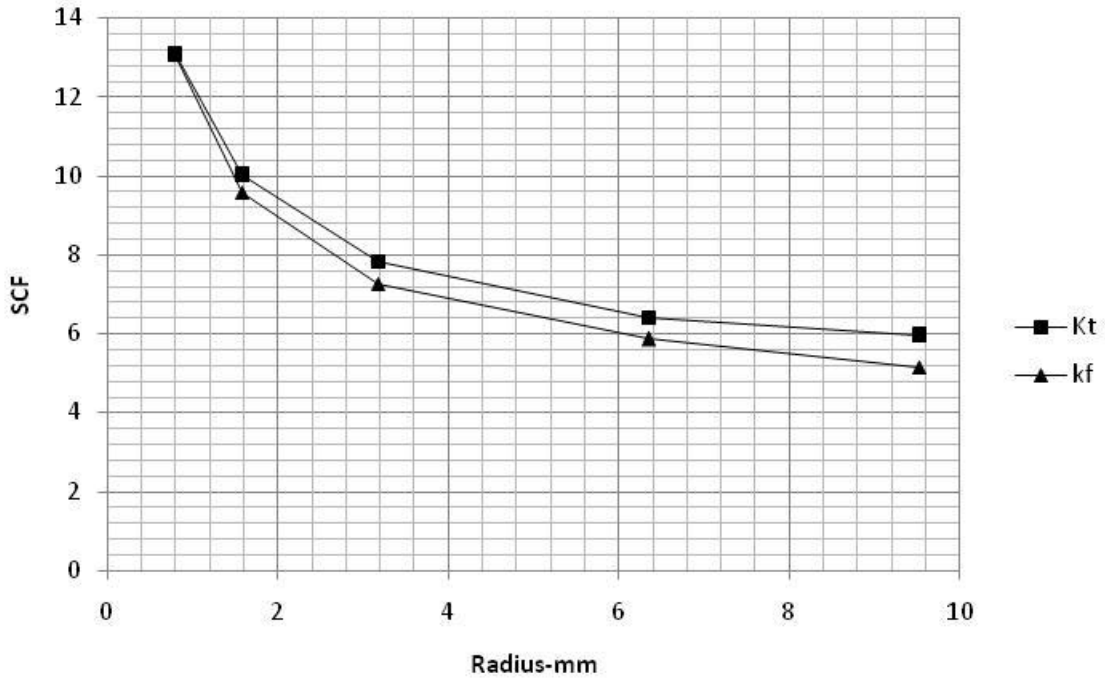

Figure 4.3 SCF vs. Radius

A graphical comparison of the two stress concentration factors listed in Table 4.2 is shown in Fig. 4.3. The figure indicates that the values of fracture stress concentration factor (K_f) is approaching to stress concentration factor (K_t) as radius of the hole decreases. The K_t value is more compared to $K_f$as the radius of the hole increases. This means, fracture mechanics approach underestimates the stress values at higher values of radius. This may be due to the stress gradient effect. LEFM approach adopts a constant stress gradient 0.5 for all radii, which is not true. From finite element studies it is observed that the stress gradient reduces from 0.439 to 0.09 as the radius increases from 0.783 mm to 9.525 mm. (Fig.4-14). This may be the reason for lesser stress prediction in fracture mechanics method. However, up to 0.25 in radius (6.35 mm) the error is less than 10%. The FE study conducted in this research work is in agreement with finite element analysis conducted by Wilson and Gabrielse (1971).

4.4 Calculation of $K_I/\sqrt{\rho}$

$K_I/\sqrt{\rho}$ is calculated for different radii to arrive at optimum radius of the hole. Eqn.4-6 is used to calculate the $K_I/\sqrt{\rho}$. The value of maximum stress at the edge of the hole is obtained from finite element analysis. Table 4-3 shows the values of $K_I/\sqrt{\rho}$ for different radius values.

$$\frac{K_I}{\sqrt{\rho}} = \frac{\sigma_y * \sqrt{\pi}}{2} \qquad (4\text{-}6)$$

Table 4-3 Calculation of $K_I/\sqrt{\rho}$ for different radii of the hole

Radius of the hole ρ (mm)	Stress σ_y (Mpa)	$K_I/\sqrt{\rho}$ (Mpa$\sqrt{mm}$)
9.56 (3/8")	245.01	217.13
6.35 (1/4")	266.03	235.76
3.17 (1/8")	327.02	289.81
1.58 (1/16")	412.2	365.30
0.79 (1/32")	539.93	478.50

According to the threshold radius given by Barsom and Rolf (1971) for given loading conditions and crack length, a crack stop hole of 0.783 mm (1/32") is necessary to prevent crack growth (see Fig.4-4)..). This is in the order of 0.01 in, which can be considered as equivalent to sharp crack with respect to crack initiation life. Therefore, according to threshold limit given by Barsom and Rolf the crack does not propagate for an applied stress of 41.2 Mpa and for a crack length of 2 inches (kept constant for all values of radius). Un-conservative prediction of $K_I/\sqrt{\rho}$ might be the one of the reason for this too small radius of the hole. To determine the accurate stress value and stress gradient N-SIF is calculated.

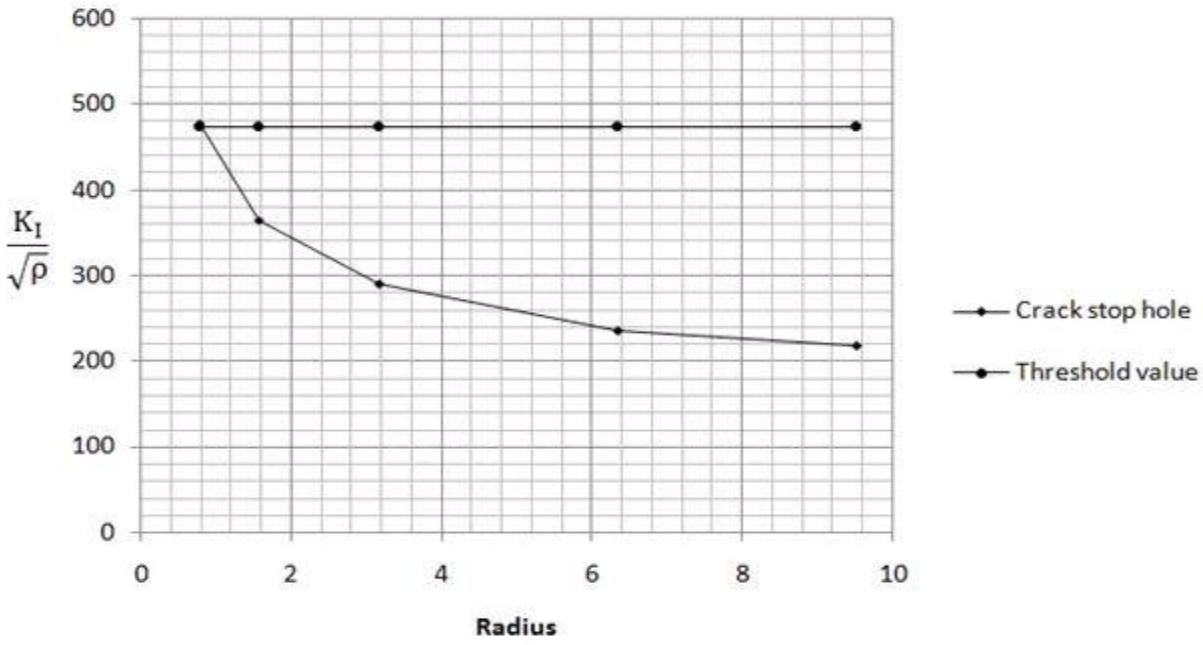

Figure 4-4 Calculation of $K_I/\sqrt{\rho}$ Values

4.5 N-SIF calculation

The literature review indicates that the crack initiation life (Ni) of a notch is typically expressed as a function of $K_I/\sqrt{\rho}$ in all studies. This $K_I/\sqrt{\rho}$ criteria is based on linear elastic fracture mechanics (LEFM). In LEFM frame work, the stress gradient ahead of the crack is expressed as a function of $1/\sqrt{r}$ singularity which indicates that when the radius approaches zero, it behaves like a sharp crack. However, the LEFM assumption is not valid if loading, crack geometry and specimen thickness leads to yielding at notch tip. In this study by keeping the geometry as same and increasing the load, the non-linear effects are studied. Three different loadings are considered from the experimental work of Fisher *et.al* (1980): 62Mpa (9 ksi), 82.7 Mpa, and 103.4 Mpa. The stress gradient (α) is calculated based on real stress distribution. The stress distribution ahead of notch tip is calculated by non linear finite element analysis. To account stress gradient and stress distribution N-SIF is calculated for each case. The concept of N-SIF is explained in chapter-3. The N-SIF expression for blunt notches is given by Boukharouba et.al (1995) Eqn.(3-11).Stress distribution for one particular case (62 Mpa loading, 9.525 mm (inch)hole radius) is explained below:

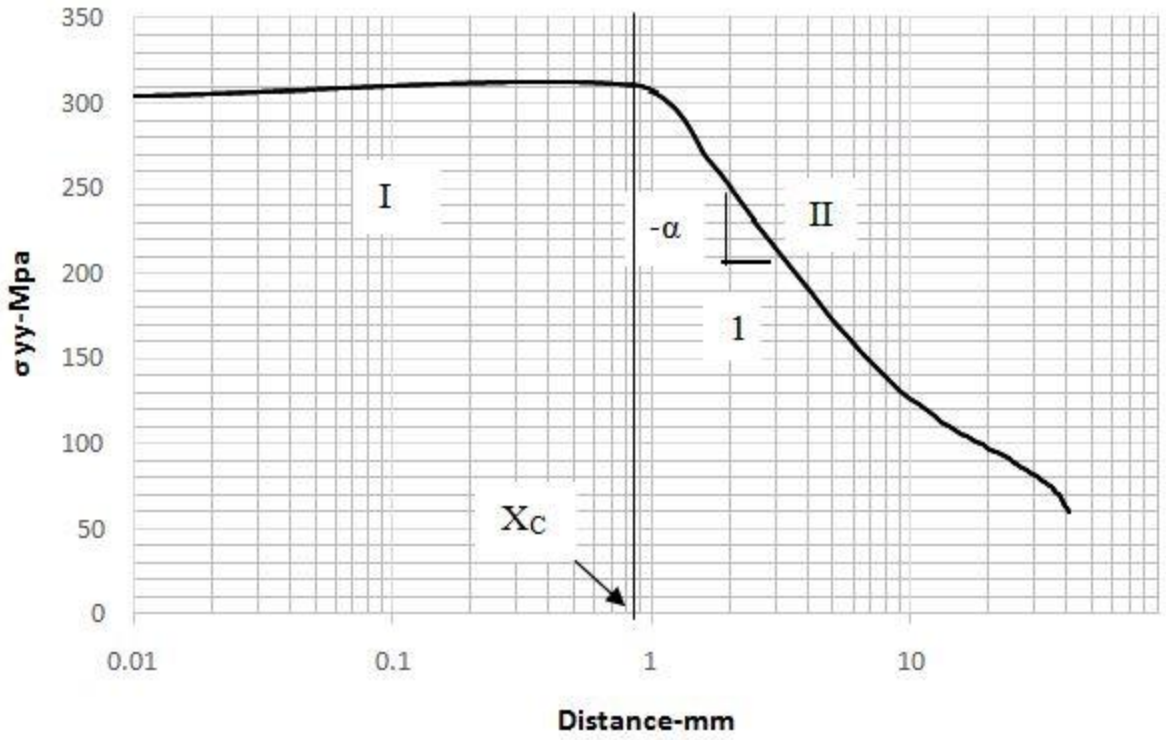

Figure 4-5 Stress distribution ahead of crack stop hole

In Fig 4-5, stress in y-direction (σ_{yy}) ahead of notch tip is plotted in semi log scale. The stress distribution is divided into three different regions. In region-I, the magnitude of stress remains same. The distance up to which stress magnitude remains constant is defined as characteristic distance (X_C). The region-II also known as pseudo singular zone, where stress distribution can be expressed as a function of N-SIF. In region-III, the stress magnitude is equal to the nominal stress.

Figure 4-6 illustrates the stress distribution ahead of crack stop hole with different radii. These results are obtained from non linear finite element analysis. The crack stop hole specimen is subjected to a tensile load of 62 Mpa (6 Ksi). This load is taken from the experimental study conducted by Fisher *et.al*(1980). The maximum stress value increases with the decrease of radius value. To calculate the values of characteristic distance (X_C), the stress value near the hole edge is plotted for three different loads (See Fig.4-7, 4-8, 4-9).

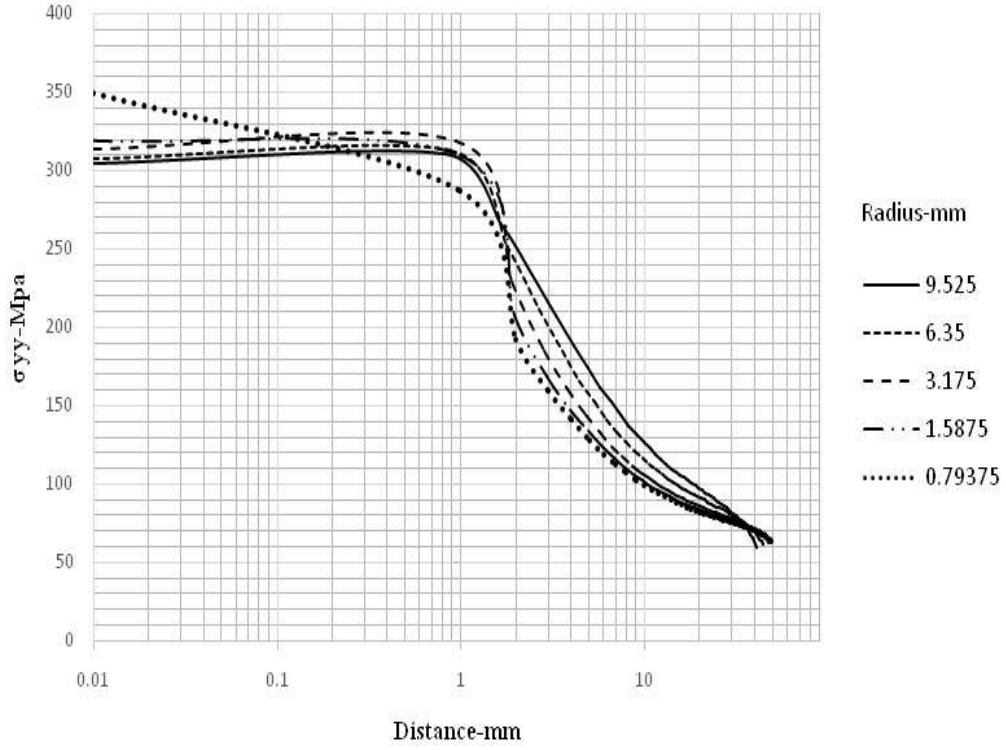

Figure 4-6 Stress distributions ahead of notch for different radii

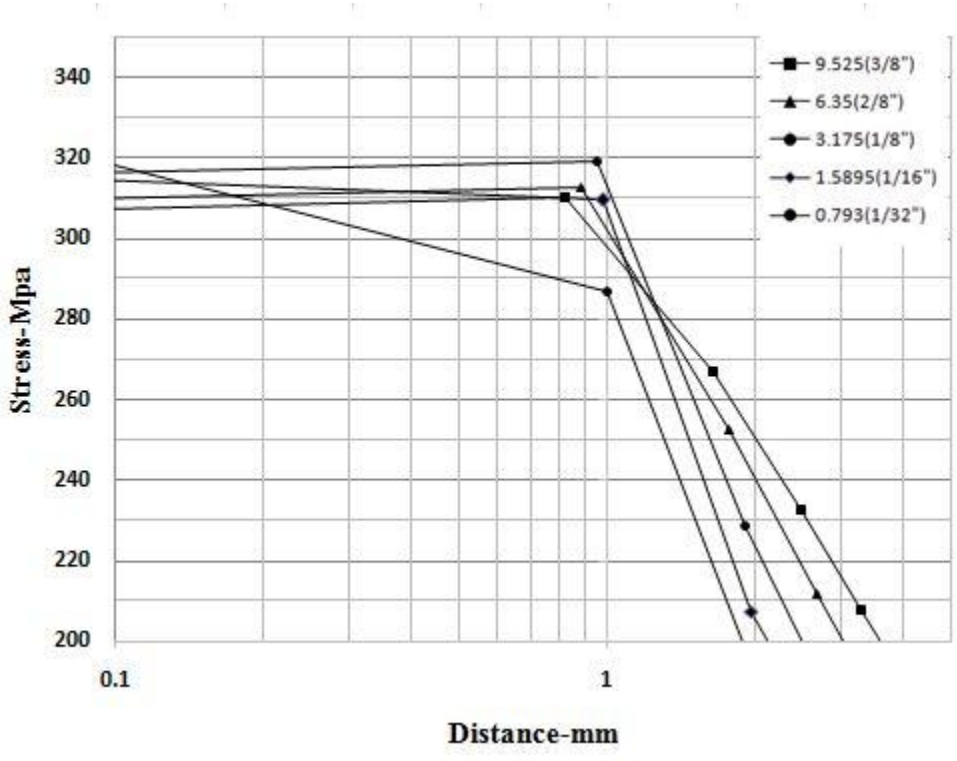

Figure4-7 Characteristic lengths (62 Mpa load)

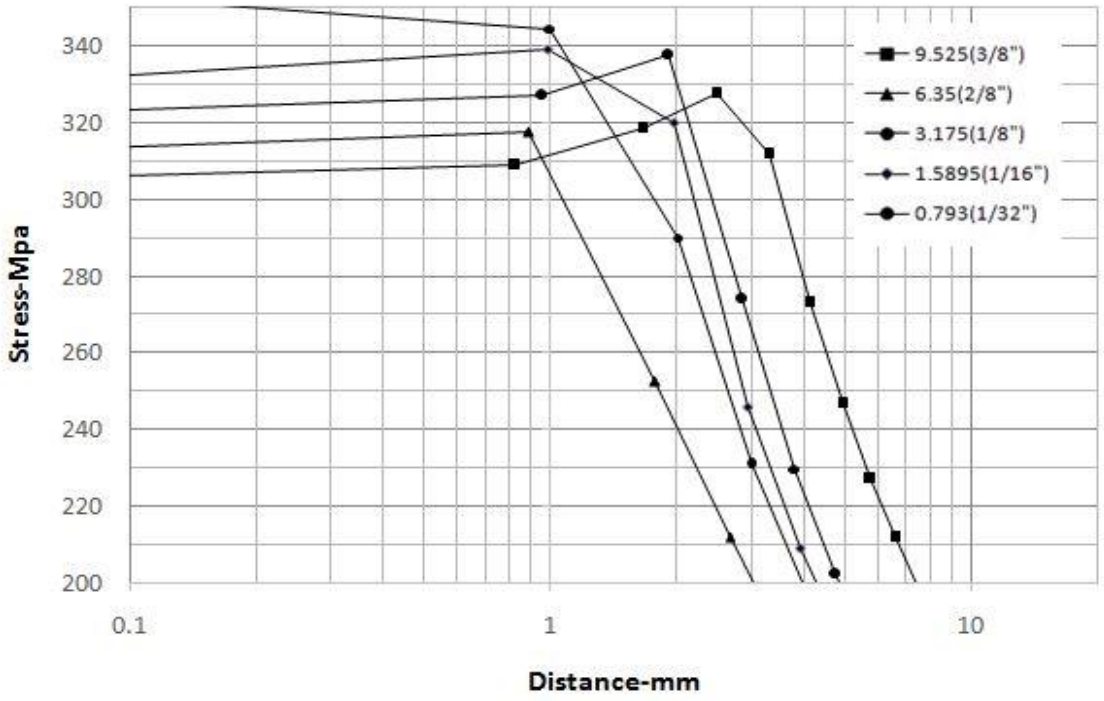

Figure 4-8 Characteristic lengths (82 Mpa load)

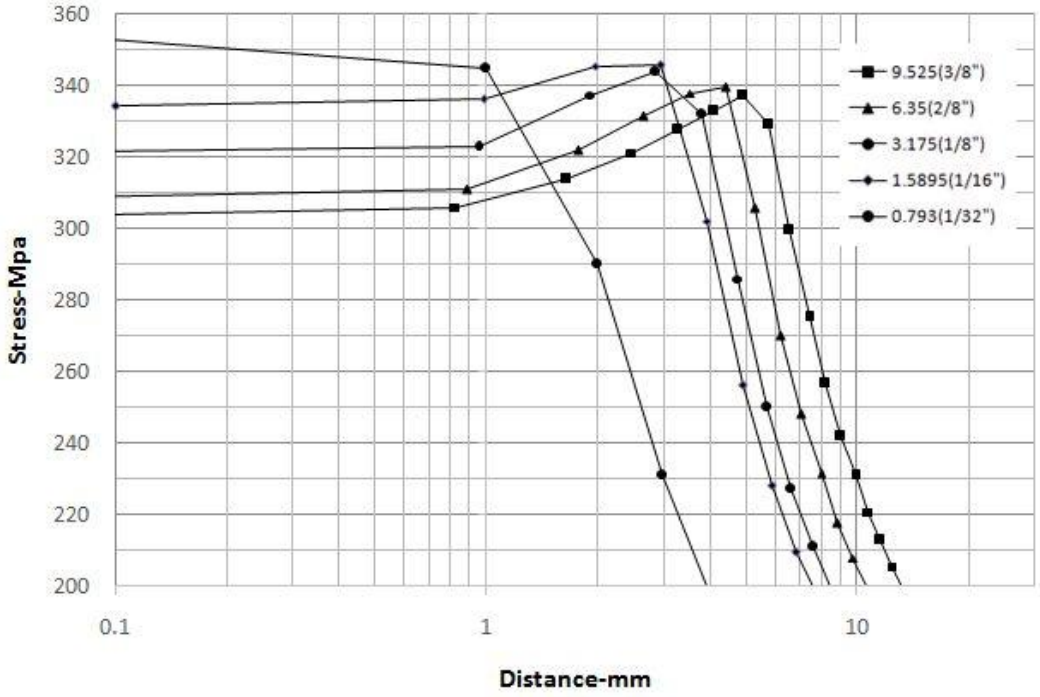

Figure 4-9 Characteristic lengths (103.4 Mpa load)

Table 4-4 Characteristic length for three loads

Load Magnitude	62 Mpa	82.7Mpa	103.4 Mpa
Radius-mm (in.)	Characteristic distance (X_c)-mm		
9.56 (3/8")	0.82	2.47	4.95
6.35 (1/4")	0.88	1.96	4.44
3.17 (1/8")	0.95	1.9	2.85
1.58 (1/16")	0.98	1.96	2.95
0.79 (1/32")	1.00	2.0	2.00

N-SIF for different radius is calculated for four applied stress based on the work done by Fisher et al.: 41.2 Mpa (6 ksi), 62 Mpa, 82 Mpa and 103 Mpa (15 ksi). The characteristic distance (X_C) is calculated for the above loading cases. Characteristic distance is defined as the distance from the edge of the hole to a point where there is a steep decrease in the stress values. The characteristic lengths are presented in Table 4-4. These values indicate that, with the load increment the characteristic length will increase. However, X_C is also varying with radius.

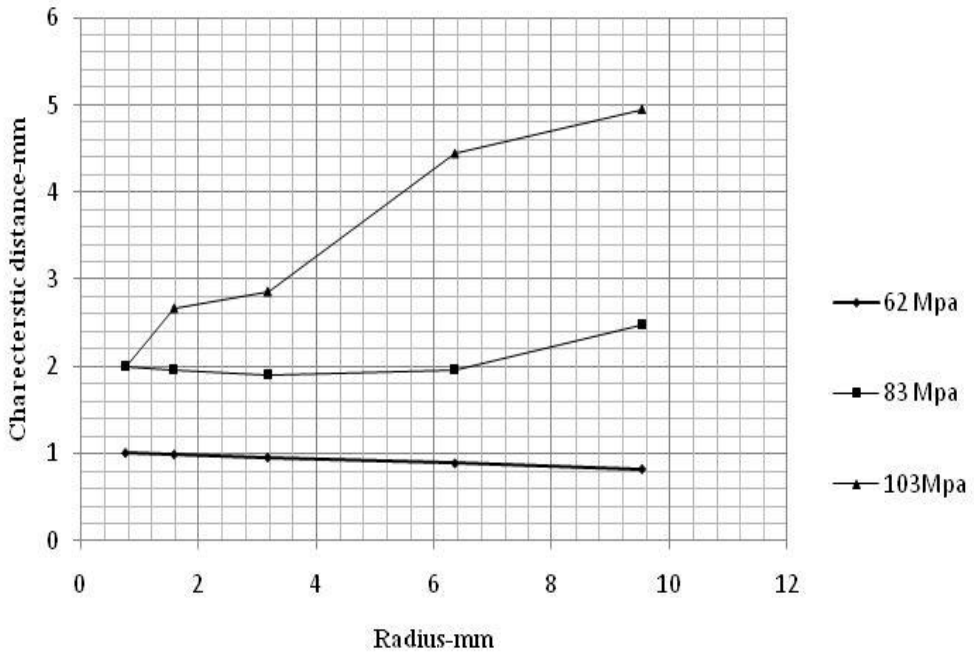

Figure 4-10 Comparison between characteristic distances

4.6 Gradient calculation(α)

The stress gradient is calculated by plotting the stress distribution ahead of the hole on a log-log scale. In the calculation of $K_I / \sqrt{\rho}$ this decrease in gradient is not considered and is assumed a constant stress gradient of 0.5 is considered for all radii.

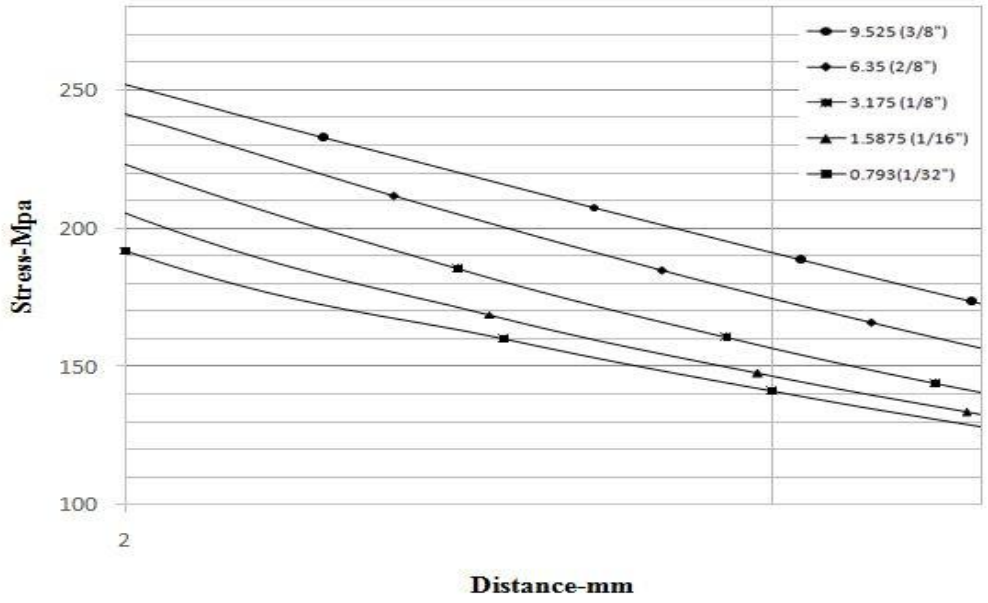

Figure 4-11Gradient for different radii (62 Mpa)

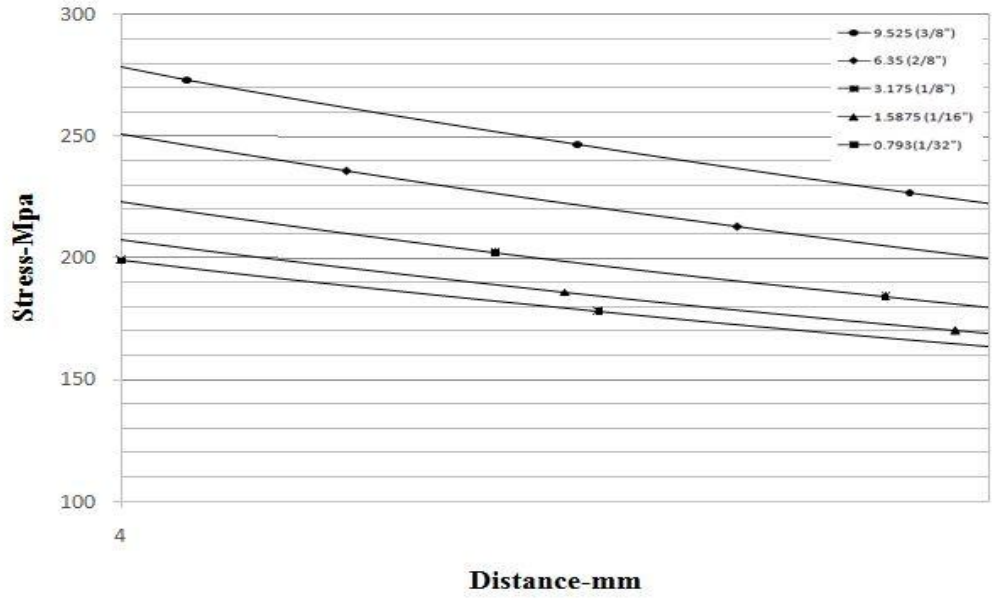

Figure 4-12Gradient for different radii (82 Mpa)

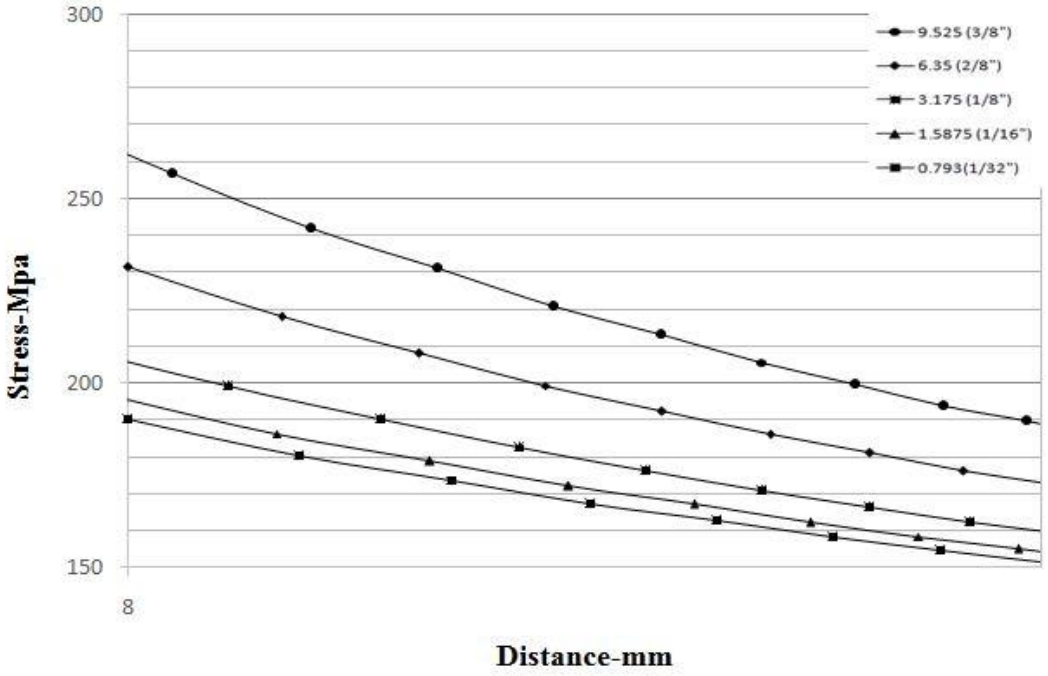

Figure 4-13 Gradients for different radii (103 Mpa)

Table 4-5 Calculation of Gradient (α)

Load Magnitude	62 Mpa	82.7Mpa	103.4 Mpa
Radius-mm(in.)	Stress gradient (α)		
9.56 (3/8”)	0.466	0.531	0.615
6.35 (1/4”)	0.437	0.484	0.52
3.17 (1/8”)	0.405	0.421	0.434
1.58 (1/16”)	0.367	0.380	0.416
0.79 (1/32”)	0.345	0.384	0.409

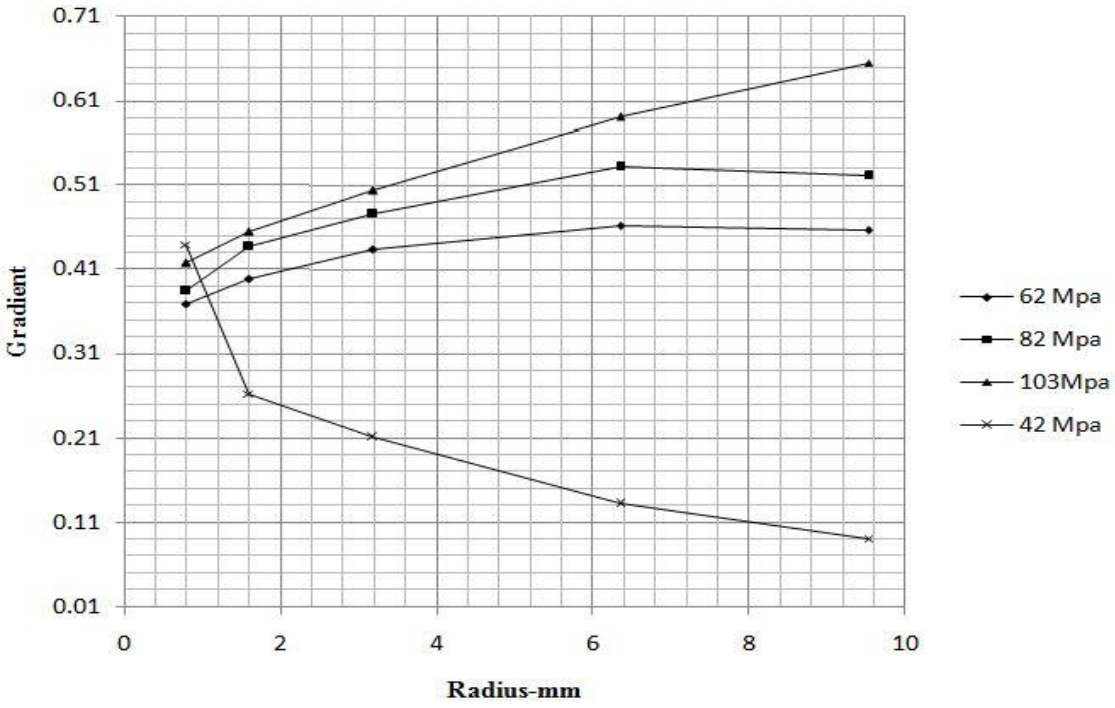

Figure4-14Gradient for different loads

4.7 Comparison between $K_I/\sqrt{\rho}$ Vs K_I/ρ^{α}

Notch stress intensity factor (N-SIF) is calculated based on the expression given by Boukharouba et.al (1995) Eqn. (3-11). In N-SIF calculation, the stress gradient and maximum stress obtained from nonlinear finite element analysis are used. It is found that the crack stop hole radius calculation based on N-SIF approach gives a radius value 4 mm (Fig.4-15) which is much greater than 1.2mm obtained from $K_I/\sqrt{\rho}$.

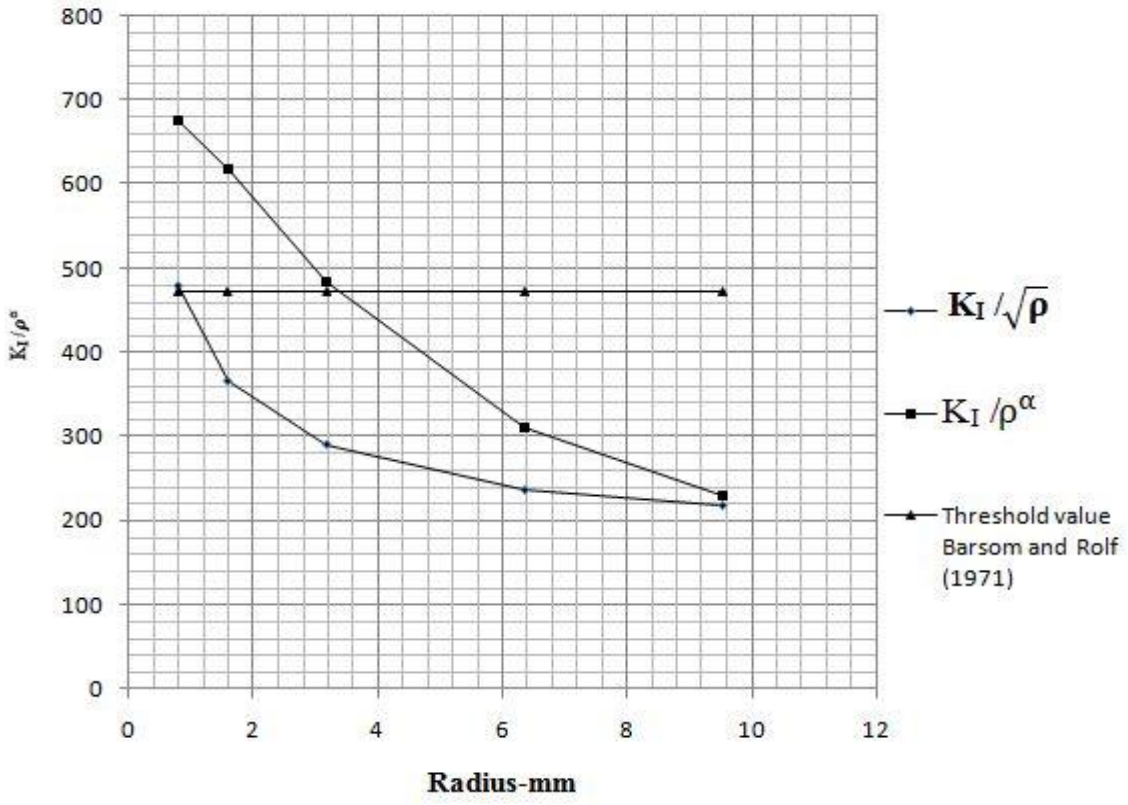

Figure 4-15 Comparison between $K_I/\sqrt{\rho}$ and K_I/ρ^α (41.2 Mpa load)

The above figures (Fig. 4.15, 4.16, 4.17, 4.18), indicates the difference between $K_I/\sqrt{\rho}$ and K_I/ρ^α for four different loads considered in this study. In each case $K_I/\sqrt{\rho}$ and K_I/ρ^α are calculated for five different radius values. These values are shown in Table 4-6.

Table 4-6 Comparison between $K_I/\sqrt{\rho}$ and K_I/ρ^α

Applied stress	**41 Mpa**	**62 Mpa**	**82 Mpa**	**103 Mpa**	**41 Mpa**	**62 Mpa**	**82 Mpa**	**103 Mpa**
Radius-mm(in.)	$K_I/\sqrt{\rho}$				K_I/ρ^α			
9.56 (3/8")	217.1	330.0	440.3	550.4	229.3	562.4	712.1	855.7
6.35 (1/4")	235.8	358.5	478.2	597.9	309.2	594.4	735.4	947.4
3.17 (1/8")	289.8	442.0	589.6	739.3	483.0	726.1	886.1	1020.2
1.58 (1/16")	365.3	549.4	732.8	916.3	616.0	836.5	1082.7	1232.1
0.79 (1/32")	478.5	719.5	959.7	1199.9	674.7	1080.4	1413.6	1556.7

4.8 Length of the Patch

Length of the patch to be used is calculated based on effective stress transfer. Different lengths of patch are analyzed. From previous studies on development length of the patch by Zhao et.al (2008) if the length of the patch exceeds a beyond a particular length, the effectiveness of patch decreases.

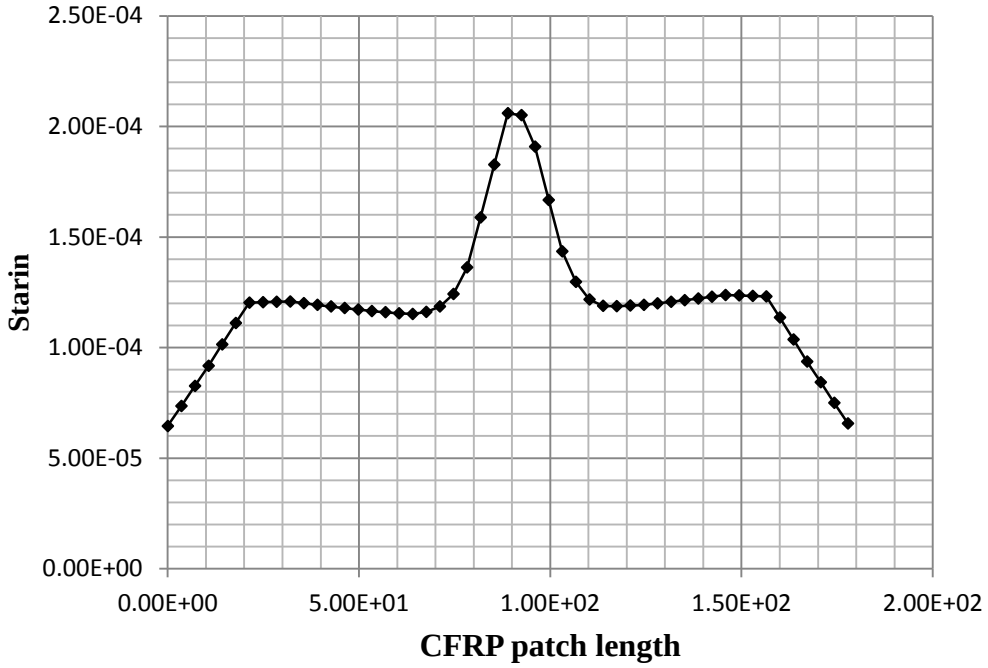

Figure4-16longitudinal strain vs. CFRP patch length

Fig 4-16 shows the variation of longitudinal strain along the length of the patch. The strain in CFRP rises sharply at the crack location. At the edges, the CFRP strain decline rapidly and this portion of length does not take part in load transfer.

4.9 Comparison between $K_I/\sqrt{\rho}$ and K_I/ρ^{α} with CFRP patch

The values of $K_I/\sqrt{\rho}$ and K_I/ρ^{α} are calculated at the edge of the hole after CFRP patch application as shown in Figs.4.20, 4-21 and 4-22.These values for three different loads are presented in Table 4-7. Also need to plot both the values for each applied stress.

Table 4-7 Comparison between KI /$\sqrt{\rho}$ and KI /ρ^{α}

Applied stress	**62 Mpa**	**82 Mpa**	**103 Mpa**	**62 Mpa**	**82 Mpa**	**103 Mpa**
Radius-mm	K_I/ρ^{α}			$K_I/\sqrt{\rho}$		
9.525	172.55	230.18	287.80	69.98	93.35	116.72
6.35	213.23	284.41	355.62	87.87	117.20	146.54
3.175	226.24	301.78	377.32	101.95	135.99	170.03
1.5875	279.41	372.69	465.99	123.92	165.29	206.66
0.793	307.17	409.72	512.28	149.90	199.95	250.00

A comparison between KI /$\sqrt{\rho}$ and KI /ρα is carried out for three different loads (62 Mpa, 82 Mpa, 103.4 Mpa) corresponding to five radii. At 62 Mpa load, for all radii, the value of KI /ρα is found to be more than KI /$\sqrt{\rho}$. In addition, it can be observed that the KI /ρα are at least 50% more than KI /$\sqrt{\rho}$ value for all radii. Same trend is observed with other two loads (82 Mpa, 103.4 Mpa).

4.10 Effect of stiffness ratio Stiffness Ratio (SR)

To study the effect of patch thickness, a parameter called stiffness ratio is introduced. The stiffness ratio is defined as the ratio of load taken by CFRP to load taken by substrate plate (AA Baker, 2002). It is assumed that the load taken by CFRP and parent metal is in the ratio of their corresponding axial stiffness's.

$$SR = \frac{t_{CFRP} E_{CFRP}}{t_{Steel} E_{Steel}} \qquad (4\text{-}7)$$

t_{CFRP}=Thickness of CFRP patch

E_{CFRP}= Young's Modulus of CFRP patch

t_{Steel}=Thickness of steel plate

E_{steel}=Young's Modulus of aluminum

.

Table 4-8 Calculation of $K_I/\sqrt{\rho}$ for different radius of the hole with patch

Value of Radius-mm						
No. of layers	SR	9.525	6.35	3.175	1.5875	0.793
2	0.16	68.80	80.78	92.61	112.06	134.29
4	0.32	46.37	58.16	67.46	81.97	99.15
6	0.48	35.92	46.16	53.85	65.74	79.82
7	0.56	32.52	41.86	49.01	59.96	72.88
8	0.64	29.80	38.47	45.00	55.16	67.10
10	0.80	25.71	33.08	38.75	47.64	58.00
12	0.96	22.73	29.10	34.15	42.05	51.21

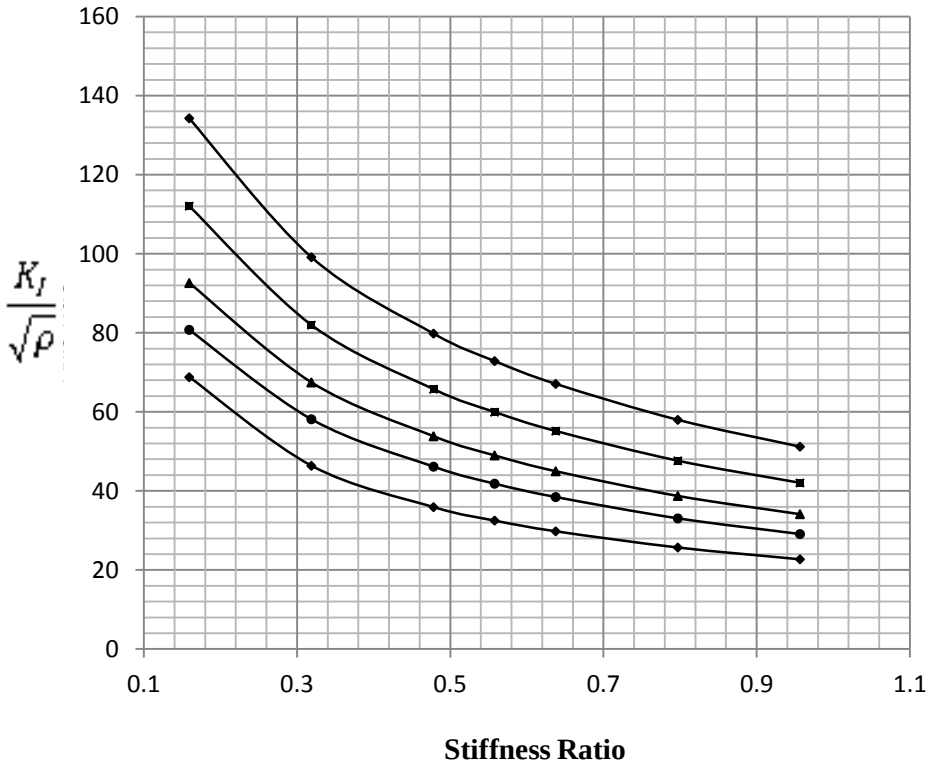

Figure 4-17 Stiffness ratio vs. $K_I/\sqrt{\rho}$

4.11 Combined action of CFRP and Crack stop hole

The combined action of CFRP patch and crack stop hole is determined by the amount of stress reduction at the edge of the hole.

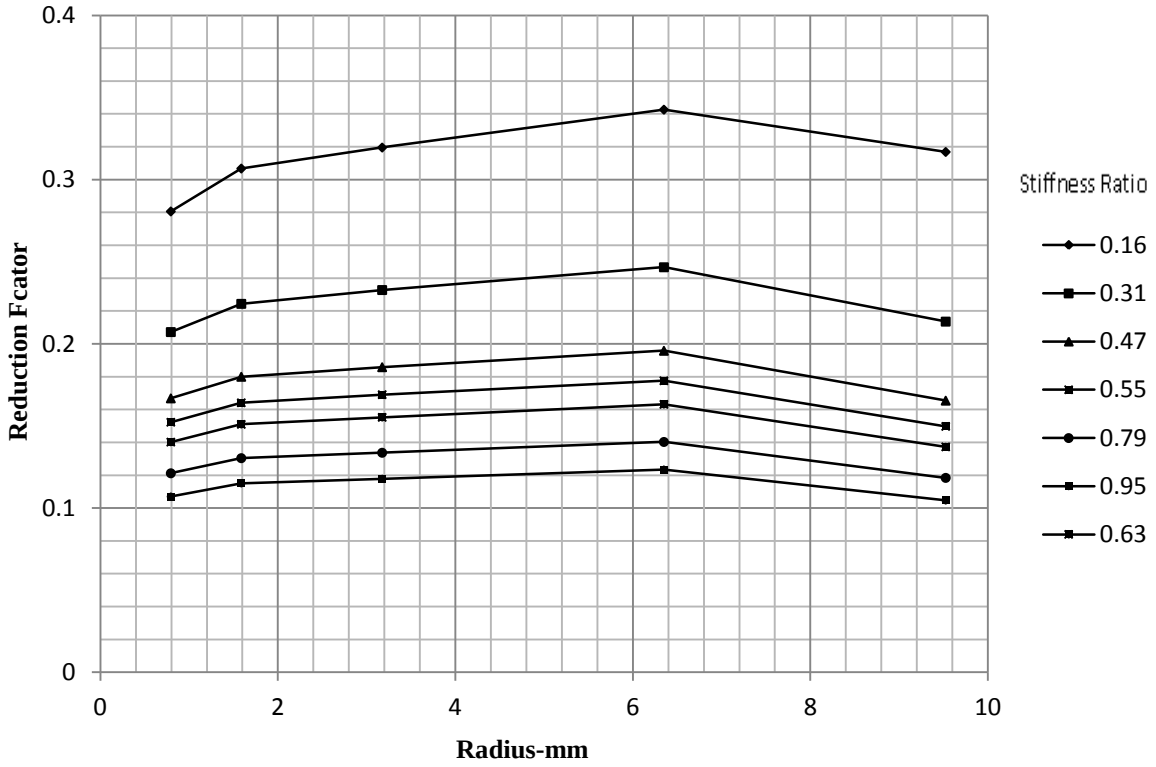

Figure 4-18 combined action of CFRP and crack stop hole

The combined action of CFRP patch and crack stop hole is studied numerically. The parameter used for comparison is $K_I / \sqrt{\rho}$. Prior studies on CFRP –steel application indicates that CFRP patches are effective in arresting the cracks initiating from notches. In thepresent study crack stop hole serves as a notch and it is assumed that the crack originates from the edge of the hole. The application of CFRP will retard the crack re initiation by reducing the stress value. CFRP patch length is taken as 150 mm. It is based on the numerical study by Zhao (2006). The effect patch thickness on reduction is calculated in terms of stiffness ratio. At a stiffness ratio 0.16, the stress value is reduced by 60%. The stress reduction becomes 90% at a stiffness ratio 0.95. Based on this study a reduction factor is introduced to the value of $K_I \sqrt{\rho}$ which is a function of stiffness ratio.

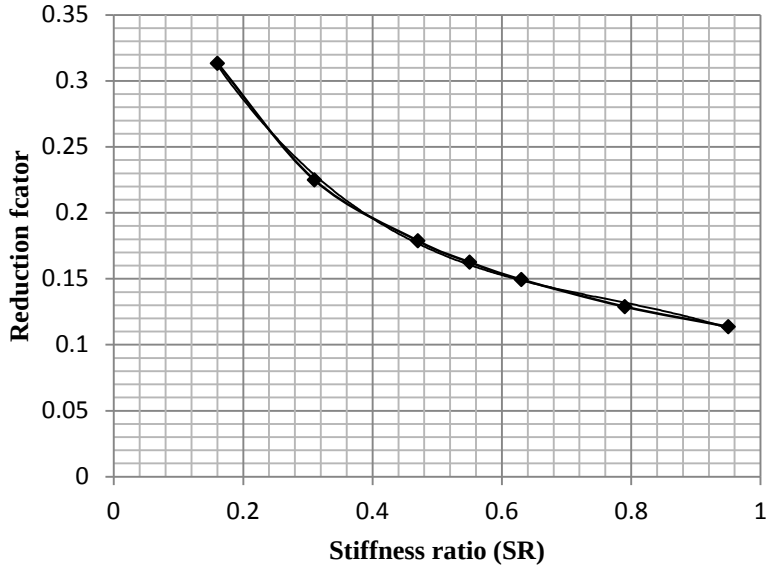

Figure4-19Stiffness ratio vs. Reduction factor

To account the effect of CFRP patch in stress reduction, a reduction factor is introduced. This factor is function of stiffness ratio (see Fig.4-19). This factor could be incorporated in the crack stop expression.

Barsom and Rolf expression:

$$\frac{\Delta K_I}{\sqrt{\rho}} = 10\sqrt{\sigma_{ys}}$$

Modified equation:

$$\frac{\Delta K_I}{\sqrt{\rho}} = \frac{10\sqrt{\sigma_{ys}}}{y}$$

Where

y= Reduction factor

Reduction factor (x) is expressed as a function of stiffness ratio

$y = -0.544(SR)^3+1.243(SR)^2-1.044\ SR+0.449$

4.12 Conclusions

The following conclusions are made from the above discussion

1. LEFM approach underestimates the stress value for larger radius value. This is due to the assumption sharp stress gradient for all radius values.
2. The crack initiation parameter ($K_I / \sqrt{\rho}$) is unconservative in predicting the crack stop hole radius compared to K_I / ρ^{α}.
3. Combined action of CFRP patch and crack stop hole will significantly reduce the stress at the edge of the hole there by increasing the fatigue crack initiation life

Chapter 5

Further study

5.1 Introduction

In this study plate with crack stop hole under tensile loading condition is considered. The type of crack studied is mode-I. This study can be further extended for other mixed loading conditions such as tensile plus torsion loading (mode I and mode III). The effect of crack stop hole and CFRP patch combination can be studied as repair technique for this combined loading case. The geometry of the crack considered in this study is central crack. An inclined crack may be considered for further study. The inclined crack creates a combination of mode-I and mode-II effect. For this mixed mode condition, the effect of crack stop hole when subjected to tensile loading can be studied. In this study it is found that power alpha gives more conservative results than $K_I/\sqrt{\rho}$. Therefore, further study is needed to arrive at a $K_I/\sqrt{\rho}$ threshold value. In addition, experimental study is needed to validate the results obtained from finite element study.

Moreover in this study, the effect of weld attachments on crack stop hole is not considered. Further study is needed to find the effect of weld attachments on crack stop hole threshold. Cracks emanating from notches needs to be studied, especially the effect of crack stops hole and CFRP on crack propagation life needs to be understand.

This study further extended to study the effect of pre stressed CFRP patches along with crack stop holes since the existing literature indicates that pre stressed patches are more efficient than normal CFRP patches.

References

1. Shield, C., Hajjar, J., Nozaka, K. (2004). “Repair of Fatigued Steel Bridge Girders with Carbon Fiber Strips,” Report no-MN/RC–2004-02, Minnesota Department of Transportation.
2. Fisher, J. W., Barthelemy, B. M., Mertz, D. R., and Edinger, J. A. (1980). "Fatigue behaviour of full scale welded bridge attachments,” *NCHR 12-15(3),* March 1980 (80-29), Fritz Laboratory Reports.
3. Jack, A.R. and Price, A.T. (1970). “The Initiation of Fatigue Cracks from Notches in Mild Steel Plates,” *International Journal of Fracture Mechanics*, 6(4), 401-409.
4. Jones, S. C., and Civjan, S. A. (2003). “Application of Fiber Reinforced Polymer Overlays to Extend Steel Fatigue Life,” *Journal of Composites Construction*, 7, 331-338.
5. Creager, M., and Paris, P. C. (1967). “Elastic field equations for blunt cracks with reference to stress corrosion cracking,” *International Journal of Fracture Mechanics*, 3(4), 247-252.
6. Crain, J., (2010). “Fatigue enhancement of undersized, drilled crack-stop holes,” Maters thesis, Kansas state university, <http://hdl.handle.net/1808/6288>.
7. Barsom, J.M., and Rolfe, S.T. (1999). *Fracture and Fatigue Control in Structures Application of Fracture Mechanics*, Third Edition. ASTM, West Conshohocken, PA.
8. Miller, C., Chajes. J., Mertz, D. R., and Hastings, J. N. (2001). “Strengthening of a Steel Bridge Girder Using CFRP Plates,” *Journal of Bridge Engineering*, 6(6), 514-522
9. Barsom, J. M. and McNicol, R. C. (1974). "Effect of Stress Concentration on Fatigue-Crack Initiation in HY-130 Steel," *Fracture Toughness and Slow-Stable Cracking*, ASTM STP 559, 183-204.
10. Andrea, M. D., Grondin, G. Y., and Kulak, G. L. (2001). “Behavior and Rehabilitation of Distortion-Induced Fatigue Cracks in Bridge Girders,” Structural Engineering Report No. 240, Department of Civil and Environmental Engineering, University of Albert, Edmonton, Albert, Canada
11. Report of Expert Group for Modernization of Indian Railways, (2012). Government of India
12. Indian railways bridge manual (1998), page 31
13. Forman, R. G. (1972). “Study of fatigue crack initiation from flaws using fracture mechanics theory,” *Engineering fracture mechanics*, 4, 333-345.
14. Wilson, W. K., and Gabrielse, S. E. (1971). "Elasticity Analysis of Blunt Notched Compact Tension Specimens," Research Report 71-1E7-LOWFA-R1, Westinghouse Research Laboratory Pittsburgh.

15. Boukharouba, Tamine, T., Niu, L., Chehimi, C., and Pluvinage, G. (1995). "The use of notch stress intensity factor as a fatigue crack initiation parameter," *Engineering Fracture Mechanics*, 52(3), 503-512.

16. Baker, A.A., Rose, L.R.F., Jones, R. (2002). *Advances in the bonded composite repair of metallic aircraft structure*, Elsevier Publications, Killington.

17. Albat, A. M., and Romilly, D. P. (1999). ''A direct linear-elastic analysis of double symmetric bonded joints and reinforcements,'' *Composite Science and Technology*. 59(7), 1127–1137.

18. Heller, M., Hill, T.G., Williams, J.F., and Jones, R. (1989). "Increasing the fatigue life of cracked fastener holes using bonded repairs," *Theoretical and applied Fracture Mechanics*, 11.

19. Fawzia, S., Al-Mahaidi, R., Zhao, X. L. (2006). "Experimental and finite element analysis of a double strap joint between steel plates and normal modulus CFRP," *Composite Structures*, 75, 156–162.

20. Achour, A.T., Bachir, Serier (2003). "Numerical analysis of the performances of the bonded composite patch for reducing stress concentration and repairing cracks at notch," *Computational Materials Science*, 28, 41–48

21. Liu, H., Xiao, Z., Zhao, X. L., Al-Mahaidi, R. (2009)," Prediction of fatigue life for CFRP-strengthened steel plates",*Thin-Walled Structures*Volume 47, Issue 10, 2009,pp 1069‑1077

22. Zhao, X. L. and Zhang, L. (2007). "State-of-the-art review on FRP strengthened steel structures," *Engineering Structures*, 29, 1808–1823.

23. Tavakkolizadeh, M. and Saadatmanesh, H. (2003). "Fatigue Strength of Steel Girders Strengthened with Carbon Fiber Reinforced Polymer Patch," *Journal of Structural Engineering*, 129, 186-196.

24. Umamaheswar, T. V. R. S. and Singh, R. (1999). "Modelling of a patch repair to a thin cracked sheet," *Engineering Fracture Mechanics*, 62, 267‑289

25. Ramji, M., Srilakshmi, R., Bhanu Prakash, M. (2012). "Towards optimization of patch shape on the performance of bonded composite repair using FEM" *Composites: Part B*, 45, 710–720

26. Alemdar, F., Gangel, R., Matamoros, A., Bennett, C., Barrett-Gonzalez, R., Rolfe, St., and Liu, H. (2013). "Use of CFRP overlays to repair fatigue damage in steel plates under tension loading," *Journal of Composite Construction.*